Geoarchaeological evidence of a buried navigable Roman canal in the Rhône delta (France): The Marius canal hypothesis

Article *in* Journal of Archaeological Science Reports · March 2025

DOI: 10.1016/j.jasrep.2025.105078

10 authors, including:

Ferreol Salomon
French National Centre for Scientific Research

Corinne Rousse
Aix-Marseille University

Grzegorz Skupinski
French National Centre for Scientific Research

Minoru Uehara
French National Centre for Scientific Research

Journal of Archaeological Science: Reports 62 (2025) 105034

Contents lists available at ScienceDirect

Journal of Archaeological Science: Reports

journal homepage: www.elsevier.com/locate/jasrep

Geoarchaeological evidence of a buried navigable Roman canal in the Rhône delta (France): The Marius canal hypothesis

Joé Juncker [a,*], Ferréol Salomon [a], Corinne Rousse [b], Grzegorz Skupinski [c], Yoann Quesnel [d], Minoru Uehara [d], Iscia Codjo [e], Nicolas Carayon [f], Benoît Devillers [g], Claude Vella [d]

[a] Laboratoire Image Ville Environnement (UMR 7362, University of Strasbourg/CNRS/ENGEES), France
[b] Centre Camille Jullian, (UMR 7299, Aix-Marseille University /CNRS), France
[c] Cultures – Environnements. Préhistoire, Antiquité, Moyen Âge (UMR 7264, University Côte d'Azur/CNRS), France
[d] Centre Européen de Recherche et d'Enseignement en Géosciences de l'Environnement, (UM 34, Aix-Marseille University /CNRS/IRD/ INRAe, Collège de France), France
[e] Archéorient-Environnements et sociétés de l'Orient ancien (UMR 5133, University Lumière Lyon 2/CNRS), France
[f] Ipso Facto, Bureau d'étude et de recherche en océanographie et en archéologie subaquatique et sous-marine, France
[g] Archéologie des Sociétés Méditerranéennes, (UMR 5140, Paul Valéry University Montpellier 3/CNRS), France

ARTICLE INFO

Keywords:
Canal
Roman hydraulic engineering
Geoarchaeology
Rhône Delta

ABSTRACT

The Marius Canal is considered the first significant Roman hydraulic infrastructure in Gaul. This navigable canal, constructed at the end of the 2nd century BCE, was located in the Rhône Delta in southern France, connecting the Rhône River to the Mediterranean Sea. In the period following the construction of the canal, the large port known as Fossae Marianae was built on the coast. Despite numerous references in ancient sources, the precise location of the canal has remained unknown for the last two millennia. However, recent geophysical surveys in the eastern Rhône Delta have revealed a linear anomaly, alongside the discovery of Roman artefacts, which may indicate the presence of a Roman canal. The objective of this study is to examine morphological, sedimentary and chronological attributes of this structure, postulated to be the Canal of Marius. Sedimentary cores extracted from the supposed canal and the banks are studied on a high-resolution scale using a detailed multi-proxy methodology (grain-size, carbonate content, organic matter, magnetic susceptibility) combined with twenty-one ^{14}C dates. The morphological analyses and palaeoenvironmental data are consistent with the hypothesis of a navigable canal operable during the Roman period, built in a complex area where an ancient lagoon was partly eroded by a palaeochannel of the Rhône dated to the 1st millennium BCE. However, further archaeological research is needed to definitely confirm that this is the canal known as the Marius Canal.

1. Introduction

Roman hydraulic engineering is recognised as among the most sophisticated during ancient times (White, 1986; Wikander, 2000; Wilson, 2012), with notable achievements including aqueducts, water mills and dams (Viollet, 2000; Grewe, 2008). This also includes navigable canals, whose remains are extremely diverse objects of study that require an interdisciplinary investigation (Purdue et al., 2015; Peter, 2021; Salomon and Rousse 2023). Existing studies show that Roman engineering was often able to take advantage of pre-existing environmental conditions (Ambert, 1998, 2000; Rousse, 2007), as illustrated by the case of the Aude Canal (Faïsse et al., 2018).

River deltas offer the opportunity to develop large navigational networks using canals to improve the connection between the sea, river channels and lagoons (Salomon and Rousse, 2022). They serve as junctions between the maritime routes and the hinterland, facilitating the transport of heavy goods (de Izarra, 1993), contributing to a high degree of interconnection never before achieved in the Mediterranean (Arnaud, 2005; Tchernia, 2011). The conquest of new provinces was then accompanied by the improvement and dissemination of procedural knowledge of Roman military engineering, manifested in particular in the excavation of navigable canals (Viollet, 2000; Leveau, 2004a;

* Corresponding author.
E-mail address: joe.juncker@live-cnrs.unistra.fr (J. Juncker).

https://doi.org/10.1016/j.jasrep.2025.105034
Received 13 June 2024; Received in revised form 4 February 2025; Accepted 5 February 2025
Available online 16 February 2025

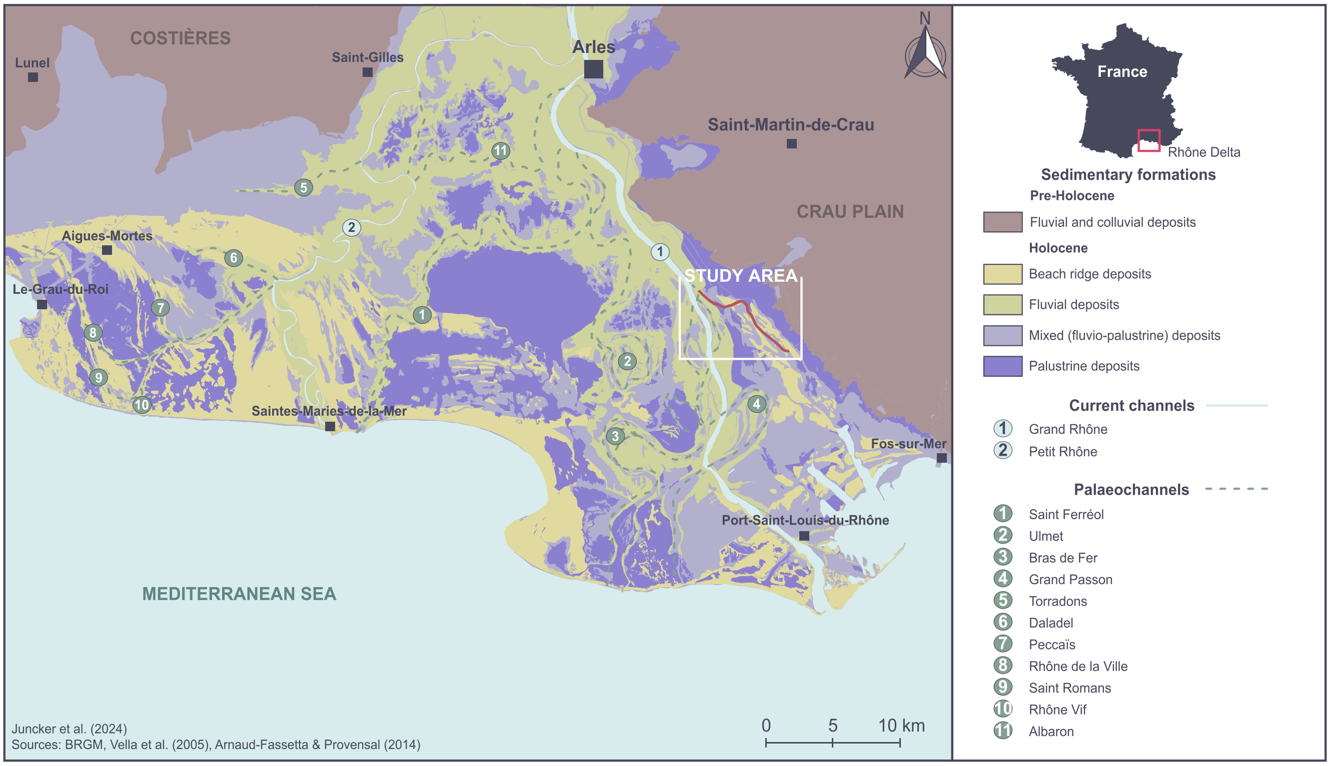

Fig. 1. The Rhône Delta.

Rousse, 2016).

Among the most important projects mentioned in ancient sources, Fossae Marianae was a canal or network of canals dug under the consul Gaius Marius between 104–102 BCE in the Rhône Delta (Strabo, n.d., *Geography*, IV,183; Pomponius Mela, n.d., *De Chorographia* II, 5, 77; Plutarch, n.d., *Marius*, XV; Pliny the elder, n.d., *H.N.*, III, 16, 120). This canal is considered as one of the oldest Roman navigable canals and also the first Roman hydraulic structure in Gaul, preceding the Pax Romana (Rousse et al., 2019). This infrastructure was crucial to better connect the Mediterranean Sea to north-western Europe and could have had an important role in the harbour system of Fos-sur-Mer from the 1st c. BCE onwards (Fontaine et al., 2019).

Following the discovery of archaeological evidence and a linear feature in the eastern part of the delta, a hypothesis for the Marius Canal has recently been proposed (Badan, 2013; Rousse et al., 2019). The aim of this study is to test if the morphological, paleoenvironmental and geochronological data are consistent with the Marius Canal hypothesis. We will attempt to determine the nature and chronology of this channel from sediment cores associated with this anomaly. These will be analysed at high resolution using sedimentological methods and a wide range of radiocarbon dates in order to assess the chronology of the canal in three main stages (Salomon et al., 2014): (1) excavation and construction; (2) the period of hydrological activity and therefore use by navigation; (3) the cessation of activity and therefore its gradual or sudden disappearance from the landscape. This study discusses an important element of water infrastructure from the Roman period, but it also provides essential elements for improving techniques to identify Roman canals, which has already made great progress in recent decades (Makaske et al., 2008; de Kort and Raczynski-Henk, 2014; Faïsse et al., 2018; Verhagen et al., 2022; Salomon and Rousse, 2023).

2. Geomorphological and archaeological context

2.1. The Rhône delta

The Rhône River has one of the largest catchment areas in Europe, spanning 97,800 km^2. The deltaic plain, covering an area of 1,800 km^2, begins between Beaucaire and Arles, where the river divides into two branches (Fig. 1) The Grand Rhône and the Petit Rhône (Brousse and Arnaud-Fassetta, 2011; Arnaud-Fassetta and Provansal, 2014). The present-day morphology of the delta is multilobed (Galloway, 1975), with a microtidal range of 20 cm (Oomkens, 1970). It is the result of a combination of marine processes, including sea-level oscillations, longshore drift and swells, in conjunction with the river's hydrological regime, vertical deformations and sediment inputs (Arnaud-Fassetta, 1998; Vella and Bourcier, 1998; Vella et al., 2005). The morphology of the deltaic plain is subject to constant change, although this may accelerate in the coming decades due to fluctuations in sediment discharge from the river and the projected rise in mean sea level (Arnaud-Fassetta and Provansal, 2014; Arnaud-Fassetta and Suc, 2015).

During the early Holocene, the rapid sea level rise caused by melting ice sheets led to a major marine transgression, flooding coasts around the world. For the lower Rhône plain, the rising sea caused the shoreline to migrate landwards, reaching almost the apex of the present delta, where sedimentary aggradation processes prevailed during this period (Vella et al., 2005; Arnaud-Fassetta and Suc, 2015). The slowdown in eustatic sea level rise that began globally between 5900 and 5000 BCE (Fleming et al., 1998; Lambeck et al., 2014; Vacchi et al., 2016), associated with changes in sediment fluxes, signalled the initiation of river delta formation around the world, including the RhôneDelta (Stanley and Warne, 1994; Vella et al., 2005; Hori and Saito, 2007). The Saint-Ferréol branch, the oldest recorded branch (L'Homer et al., 1981, Arnaud-Fassetta, 1998), carrying a large amount of alluvium, was at the origin of a slow progradation phase in the central compartment (Fig. 1) around 4500 BCE (Provansal et al., 2003, Arnaud-Fassetta, 1998). The deltaic plain continued to grow as progradation continued, still

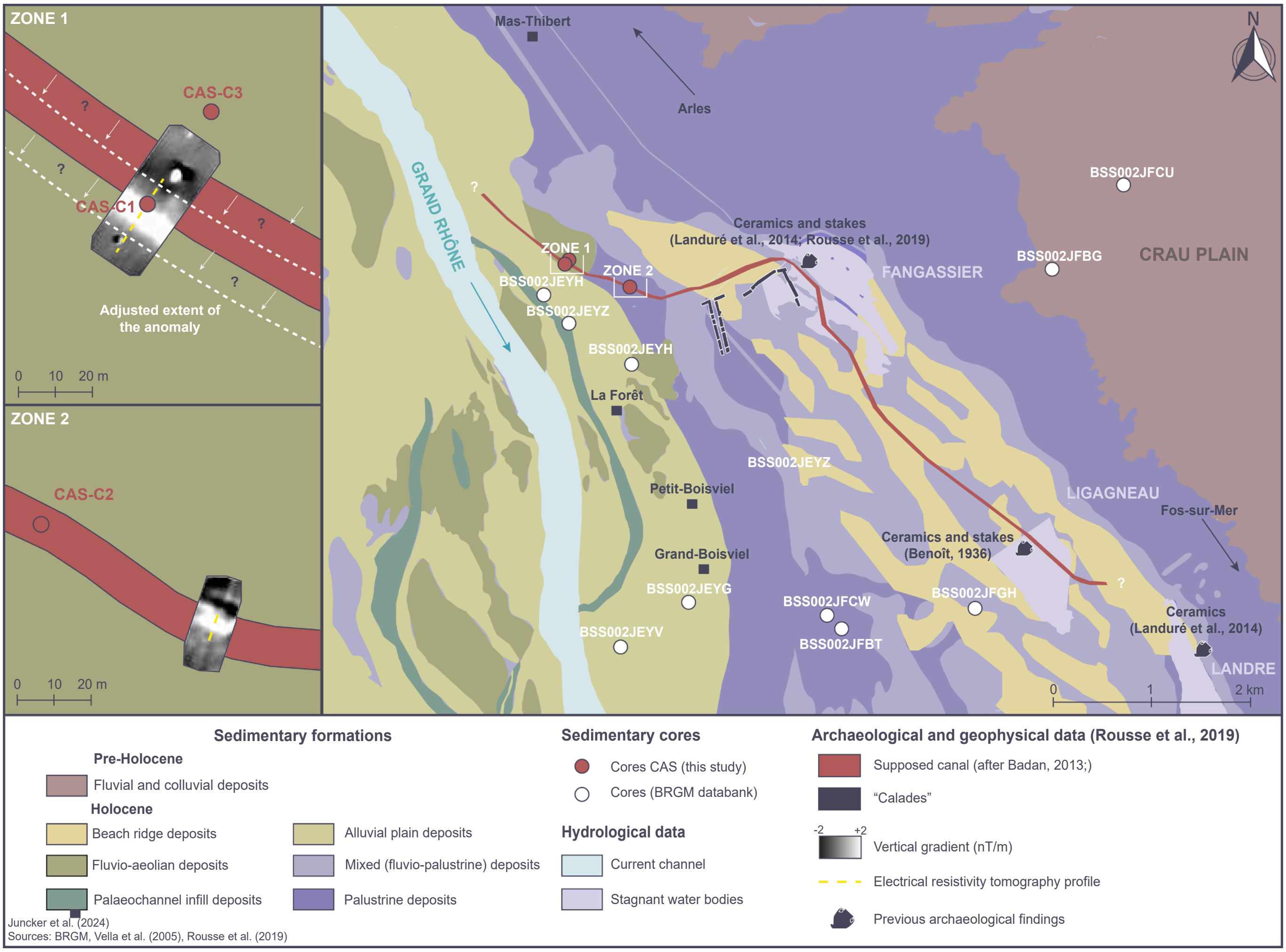

Fig. 2. Study area. (See above-mentioned reference for further information.)

benefiting from the slowdown and the stabilisation of the sea level. The Ulmet channel, located in the east of the delta, is the second oldest dated branch and was active around 3830 BCE (Vella et al., 2005). In accordance with historical sources (Tréziny, 2004), three Rhodanian branches may have been active around 100 BCE. Geomorphological studies have identified these as the Saint-Ferréol, Ulmet and Daladel palaeochannels (Vella et al., 2016). Increase in sediment production due to favourable climatic conditions was observed in the delta (Arnaud-Fassetta and Landuré, 1997; Provansal et al., 1999) and further upstream in the lower river valley (Bruneton et al., 2001). The lobe gradually developed cuspate and elongated characteristics under conditions of accelerated progradation, extending beyond the current coastline at Saintes-Maries-de-la-Mer (Vella et al., 2005; 2008).

In the eastern part of the delta, the Holocene deltaic formations developed on the extension of the Crau Plain, composed of conglomerates from the ancient Durance basin (Colomb and Roux, 1978; 1986). This complex topography shaped by Durancian materials has a major influence on the current morphosedimentary dynamics. Furthermore, the east–west orientation of this geological formation declines from about 10 m b.s.l. in the Vigueirat Marshes to 30 m b.s.l. near the Lagoon of Vaccarès (Vella and Provansal, 2000; Vella et al., 2005). This altimetric variation marks a subtle but crucial transition in the morphology of the delta, highlighting the interactions between natural forces, such as marine currents and sediment deposition, and anthropogenic influences. Nevertheless, the eastern sector of the delta remains a challenging area to comprehend. As illustrated on geological maps, the extensive strip situated between the Crau Plain and the Grand Rhône channel displays a gradual transition from west to east, characterised by fluvial deposits, beach-ridges and marshes along the Crau plain (Fig. 1). In the scientific literature, the closest studied and dated cores were drilled 6 km to the south-east in the Viguerait Marshes and in close proximity to the Ulmet branch, 5 km to the west (Vella, 1999). Other cores that have been studied are located upstream of Arles on the right bank. These include the Augery core, which was drilled at a distance of 10 km (Pons, Toni and Triat, 1979), and the Arles-Piton core, which was drilled at a distance of 20 km to the north (Arnaud-Fassetta et al., 2005). The closest cores are those collected by the *Bureau de Recherches Géologiques et Minières* (BRGM) but with only concise descriptions of the stratigraphic units (Fig. 2).

2.2. *Fossae Marianae: Canal and port of Arles*

The Marius Canal was excavated during an episode of the Cimbrian Wars, following the long migration of Cimbres and Teutons from Jutland (Denmark) around 120 BCE, which threatened the hegemony of the Roman Republic (Luginbühl, 2014). Although the causes of the migration of these tribes are not fully understood, it has been suggested that climatic crises may have been a contributing factor (Demougeot, 1965; Compatangelo-Soussignan, 2016). We know that the war ended with the defeat of the Germanic tribes in 101 BCE at Vercelli (Donnadieu, 1954). This lateral canal was dug to supply Marius' troops stationed around Arles between 104–102 BCE (Strabo, n.d., *Geography*, IV,183; Plutarch, n.d., *Marius*, XV; Pliny the elder, n.d., *H.N.*, III, 16, 120) and connected the Rhône to the Mediterranean bypassing the natural river mouths of the Rhône and their bars. Upon his return to Italy, G. Marius bequeathed the canal to Marseille, which, according to Strabo (*Geography*, IV,183), benefited from it by imposing taxes on maritime trade. It seems likely that the canal was offered to Arles following the siege of Marseille during the civil war in 49 BCE (Collin Bouffier, 2009). The colony of Arles, established in 46 BCE, encompassed a significant portion of Marseille's territory, which could be another reason for a change in ownership (Leveau, 2004b). The construction of the canal(s) led to the development of a large port complex at the seafront around 20 BCE (Liou and Sciallano 1989; Fontaine et al., 2019). This port complex was known by various sources from the 2nd c. CE under the name of Fossae Marianae (*Antonine Itinerary*, 299; *Maritime Itinerary*, 507; *Peutinger Table*). These two structures constituted the outport of Arles (Leveau, 2004b; Fontaine et al., 2019), an important metropolis of the Rhône corridor, situated at a crossroads of a maritime and fluvial trade networks (Benoît, 1964; Leveau, 2014; Long and Duperron, 2016; Djaoui, 2017). The cessation of activity is occasionally dated to the late 1st c. CE, since Pliny, who lived during that period, is the last source to mention the canal (Pliny the elder, n.d., *H.N.*, III, 16, 120; Lugand, 1926). Although the exact reasons for the abandonment are unknown, hydro-sedimentary variations have often been suggested based on ancient sources. For example, the hypothesis that a mouth bar was present and prevented ships from travelling upstream would have been one of the reasons for the construction of the canal. If this obstacle disappeared, it could have made the canal obsolete according to some scholars (Vella et al., 1999; Marlier, 2018). However, the port of Fos continued to be active until the beginning of the 3rd c. CE (Fontaine et al., 2019).

The location of the canal and associated structures is still debated (Vella et al., 1999; Leveau and Trousset, 2000). Since the 19th c., many scenarios have been proposed for its route. Some of them suggested a connection with the present Grand Rhône (Véran, 1808; Desjardins, 1876) or with the Ulmet palaeochannel (Clerc, 1906). Matheron (1825) mentions the existence of ditches, platforms, walls and paths as well as the locations of the 'ancient towns' and the entrenched camps of Marius. An excavation of the channel through the lagoons and marshes of the delta has also been proposed (Saurel, 1865; L'Homer et al., 1981). Building upon research proposals by Vella et al. (1999), Badan (2013) formulated a new hypothesis regarding the Marius Canal in the Vigueirat Marshes after discovering a buried feature through manual penetration tests (Fig. 2). The morphology was later confirmed by geophysical surveys (Fig. 2; Rousse et al., 2019), one of the first approaches in the search for ancient canal traces (Salomon and Rousse, 2023). Multiple archaeological findings strongly support Badan's hypothesis. In the vicinity, archaeologists discovered 69 ceramic fragments dating to the late 1st c. BCE (Rousse et al., 2019). In addition, two *Abies alba* stakes have been found later. Radiocarbon dating placed these stakes within the Roman period: Stake P1 (Ly-16580) dated to 4–131 CE and Stake P2 (Ly-16581) to 131–326 CE (Landuré et al., 2014; Rousse et al., 2019). Furthermore, two substantial cobbled platforms, measuring between 30 000 and 40 000 m^2, were identified south of the canal with materials dated from the 1st c. BCE to the 3rd c. CE exclusively (Rousse and Marty, 2023), providing additional evidence for significant Roman activity in this area.

3. Material and methods

3.1. Fieldwork

Drilling campaigns were carried out in July 2020 and September 2021 in the nature reserve of the Vigueirat Marshes. The cores were placed in collaboration with O. Badan and using previous geophysical results. Furthermore, a preliminary assessment of the anomaly's width was conducted in the two identified zones using a hand auger. Three cores were drilled through the use of an Atlas Copco Cobra TT machine with a closed core sampler for polyvinyl chloride (PVC) sample tubes. The extraction process was conducted using a Stitz hydraulic lifter in conjunction with a Honda EC 3800 generator. The elevation is determined in accordance with the French national system, the Nivellement Général de la France (NGF), through a global navigation satellite system (GNSS) comprising two Trimble R8 antennas (Table 1).

Table 1
Details of the CAS cores.

Core	Zone	Position	Elevation (m a.s.l.)	Depth (m)	X-Y (EPSG 3857)
CAS-C1	1	In the supposed canal	2.08	9.80	527454–5393422
CAS-C2	2		1.47	8	528362–5393101
CAS-C3	1	Out of the supposed canal	1.55	9	527501–5393483

Table 2
Details of identified malacofauna.

Core	Elevation (m)	Species	Number	Environment
CAS-C1	7.76 b.s.l.	*Cerastoderma edule*	1	Infralittoral - Superficial muddy sands in calm waters
	3.69 b.s.l.	*Theodoxus fluviatilis*	1	Fluvial
		Radix auricularia	1	
CAS-C3	5.96 b.s.l.	*Lentidium mediterraneum*	9	Infralittoral - High-level fine sands
		Bornia Sebetia	2	Infralittoral - Superficial muddy sands in calm waters
		Bornia sebetia	1	
		Loripes orbilatus	1	
		Diplodonta intermedia	1	
		Cerastoderma glaucum	1	
		Parvicardium scriptum	2	Infralittoral -Euryhaline lagoon biocenosis
		Cerastoderma edule	1	Infralittoral - Superficial muddy sands in calm waters
		Loripes orbiculatus	8	
	2.96 b.s.l.	*Loripes orbiculatus*	1	
	1.20 b.s.l.	*Bornia sebetia*	1	

3.2. Palaeoenvironmental analyses methods

Visual inspection and initial stratigraphic description were carried out once cores were opened. Magnetic susceptibility was measured every centimetre in SI units using a Bartington MS2K sensor adapted for magnetic stratigraphy in sedimentology (Dearing, 1999). After measurement, the cores were sampled to a resolution of 3 cm and adjusted to stratigraphic units. The intact shells were extracted from the visible stratigraphy and the species were then determined using references for the Mediterranean Sea (Cossignani and Ardovini, 2011; D'Angelo and Gargiullo, 1978)), as well as the World Register of Marine Species (WoRMS). Subsequently, the environment was identified (Table 2) based on the works of Pérès and Picard (1964), Bellan-Santini et al. (1994) and Michez et al. (2014).

Three sedimentological analyses were conducted on CAS-C1 and CAS-C3. The grain-size was analysed using a Coulter Beckmann LS230 laser particle sizer consisting of an optical laser bench combined with a fluid module (1.7 l) or a dry module (loose and mainly sandy sediments). The detection range extends from 0.04 μm to 2000 μm over 117 classes of particles. The sample preparation protocol was based on the specific

Table 3
Summary of the AMS radiocarbon dates.

Core	Elevation (m)	Lab. sample	Dating support	^{14}C yr B.P.	Age calibrated BCE/CE-2σ (Reimer et al., 2020)
CAS-C1	7.83b.s.l.	BETA No 567,835	Plant mat.	6480 ± 30	5481–5371 BCE (95.4 %)
	7.45b.s.l.	Lyon 18,889	Wood	2570 ± 30	808–749 BCE (73.0 %) 686–666 BCE (6.9 %) 639–569 BCE (15.6 %)
	6.45b.s.l.	Lyon 18,888		3400 ± 30	1886–1852 BCE (2.0 %) 1769–1615 BCE (93.4 %)
	5.75b.s.l.	Lyon 18,887		2810 ± 30	1050–897 BCE (93.5 %) 870–849 BCE (1.9 %)
	5.20b.s.l.	Lyon 18,886		3150 ± 30	1500–1383 BCE (87.0 %) 1341–1314 (8.5 %)
	4.43b.s.l.	Lyon 18,885		2310 ± 30	413–354 BCE (78.7 %) 285–229 BCE (16.7 %)
	4.43b.s.l.	Lyon 18,884		2510 ± 30	786–541 BCE (95.4 %)
	3.69b.s.l.	BETA No 567,834		4830 ± 30	3651–3599 BCE (42.5 %) 3590–3528 BCE (53.0 %)
	3.34b.s.l.	Lyon 18,883		2250 ± 30	392–347 BCE (30.5 %) 315–204 BCE (64.9 %)
	2.81b.s.l.	Lyon 18,882		2300 ± 30	409–353 BCE (70.2 %) 286–228 BCE (24.6 %) 217–211 BCE (0.7 %)
	2.14b.s.l.	Lyon 18,881		2155 ± 30	355–281 BCE (32.2 %) 231–93 BCE (59.6 %) 75–55 BCE (3.3 %)
	1.1b.s.l.	BETA No 567,833	Charcoal	2030 ± 30	147–140 BCE (0.6 %) 108 BCE-69 CE (94.8 %)
	0.47b.s.l.	Lyon 18,880	Plant mat.	463 ± 30	1410–1464 CE (95.4 %)
CAS-C2	6.24b.s.l.	Lyon 18,894	Wood	6620 ± 30	5620–5481 BCE (95.4 %)
	5.73b.s.l.	Lyon 18,893		6395 ± 30	5474–5428 BCE (26.3 %) 5416–5309 BCE (69.2 %)
	4.05b.s.l.	Lyon 18,892		2360 ± 30	540–527 BCE (2.3 %) 521–386 BCE (93.1 %)
	2.2b.s.l.	Lyon 18,891	Plant mat.	3435 ± 30	1876–1842 BCE (14.9 %) 1823–1796 BCE (6.6 %) 1780–1629 BCE (74.0 %)
	0.57 a.s.l.	Lyon 18,890	Charcoal	930 ± 30	1032–1178 CE (93.2 %) 1192–1203 CE (2.3 %)
CAS-C3	4.87b.s.l.	LTL22588	Wood	6050 ± 40	5201–5186 BCE (1.6 %) 5053–4837 BCE (93.9 %)
	4.38b.s.l.	LTL22587	Plant mat.	5805 ± 40	4781–4750 BCE (4.9 %) 4729–4545 BCE (90.6 %)
	2.34b.s.l.	LTL22586		3036 ± 40	1412–1197 BCE (92.9 %) 1173–1163 BCE (1.1 %) 1143–1131 BCE (1.5 %)

expertise of the laboratory and is as follows. The organic matter was initially destroyed by an attack with hydrogen peroxide (H_2O_2). Subsequently, the flocculent ions were eliminated by washing with potassium chloride (KCl). Finally, the sample was dispersed with sodium hexametaphosphate ($Na_6P_6O_{18}$) under rotary agitation for a period of between four and six hours before measurement.

The concentration of carbonates was determined by employing a Bernard calcimeter following the methodology outlined by Hoffmann and Pellegrin (1997) around 20 °C. This involved releasing a specified volume of CO_2 upon contact with hydrochloric acid (HCl), proportional to the amount of calcium carbonate ($CaCO_3$) present. Greater $CaCO_3$ quantities result in more CO_2 release, visible through the graduated cylinder. Controls were run every 10 samples to quickly identify and rectify any deviations.

Organic matter content was estimated using the loss-on-ignition method, which measures weight loss after calcining dry samples at 375 °C for 16 h. This temperature was specifically chosen to accurately quantify soil organic matter by minimising the loss of structural water from clays and preventing the release of CO^2 from carbonates or the decomposition of elemental carbon. By operating at 375 °C, the method reduced errors associated with inorganic weight loss and gave results comparable to those obtained by chemical analysis, ensuring a reliable assessment of organic matter content (Ball, 1964).

3.3. Radiocarbon dating strategy

Selected materials in the cores were dated by radiocarbon (Table 3). Priority was given to sampling from deposits that could be associated with the anomaly (Figs. 3, 5 and 6). Subsequently, the remaining samples were distributed across the various stratigraphic units, ensuring comprehensive coverage of the depositional environments across all time periods. With regard to the type of dated material, terrestrial materials were selected, with wood and charcoal extracted from the cores to prevent contamination at the tube extremities. In exceptional cases, plant parts were also included if the deposits were considered crucial for dating purposes. The organic samples were subjected to a cleansing process involving the use of distilled water, with the objective of eliminating any residual pollutants and mineral particles. Given the limited availability of material, we opted to employ the accelerator mass spectrometry (AMS) dating method, which is well suited to very small samples and offers a rapid and more precise alternative to conventional ^{14}C measurements. They were sent to three laboratories: The Centre de datation par le radiocarbone (Lyon, France), the Beta Analytic laboratory (Miami, USA) and the Centro di fisica applicata, datazione e diagnostica (Lecce, Italy). Calibrations were performed using the OxCal software (Ramsey and Lee, 2013) with the IntCal20 curve (Reimer

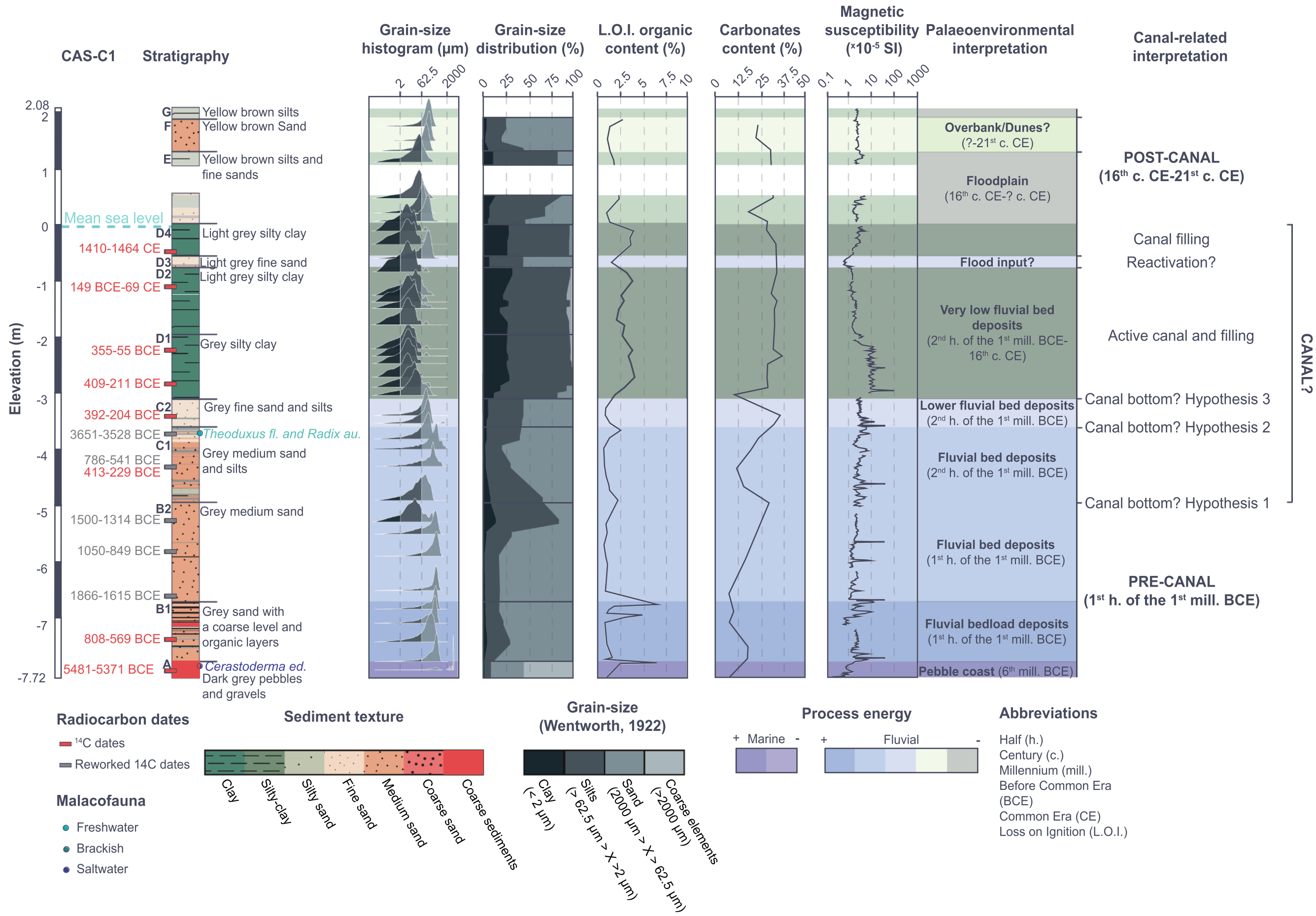

Fig. 3. Palaeoenvironmental diagram of CAS-C1. (See above-mentioned reference for further information.)

et al., 2020), with ages conventionally reported at 2 σ (i.e., 95 %).

4. Results

4.1. Hypothesised canal (Zone 1) – CAS-C1

CAS-C1 consists of five main units (Fig. 3).

Unit A (7.55–7.72 m b.s.l.) is composed of dark grey gravels and medium sands with shell fragments. *Cerastoderma edule* is present. A trapped plant material has been dated from 5481 to 5371 BCE. The organic matter content is low (0.6 %). The carbonate content is low (9–10 %). The magnetic susceptibility is low (1×10^{-5}SI).

Unit B1 (6.59–7.55 m b.s.l.) consists of an alternation of grey medium sands with 6 thin organic layers corresponding to organic matter peaks (5–7 %). A piece of wood has been dated from 808 to 569 BCE. A level of pebbles is also recorded in the middle of the unit. The carbonate content is moderate (7–14 %). The magnetic susceptibility varies strongly (0.8–50 x10^{-5}SI).

Unit B2 (4.82–6.59 m b.s.l.) is composed of grey medium sands and silts. Three pieces of wood have been dated from 1886 to 1645 BCE, from 1050 to 849 BCE, and from 1500 to 1314 BCE respectively. The organic content remains low (1–2 %). The carbonate content increase from the base to the top (12–25 %). The magnetic susceptibility varies strongly (1–60 x10^{-5}SI).

Unit C1 (3.51–4.82 m b.s.l.) consists of grey medium sands and silts. *Theodoxus fluviatilis* and *Radix auricularia* are present. Three pieces of wood have been dated from 413 to 229 BCE, from 786 to 541 BCE and from 3651 to 3528 BCE and from 392 to 204 BCE respectively. The organic content remains low (2 %). The carbonate content first decreases (12 %) before increasing to the top (28 %). The magnetic susceptibility is still very variable (1–70 x10^{-5}SI).

Unit C2 (3.04–3.51 m b.s.l.) is composed of grey well-sorted fine sand with silty layers. A piece of wood has been dated from 392 to 204 BCE. The organic content is low (around 2–3 %). The carbonate content is higher (37 %). The Magnetic susceptibility is high at the base (60x10^{-5}SI) before becoming stable on lower intensities (4x10^{-5}SI).

Unit D1 consists of grey clayey-silty sediments. Two pieces of wood have been dated from 409 to 204 BCE and from 355 to 55 BCE respectively. The organic content increases compared to previous units (3–4 %). The carbonate content is high and stable (27 %). The magnetic susceptibility is very high (15-105x10^{-5}SI) which corresponds well with the surface magnetic anomaly (Fig. 4).

Unit D2 consists of grey clayey-silty sediments. A charcoal has been dated from 147 BCE to 69 CE. The organic content is similar the previous unit (2.5–5 %). The carbonate content is slightly higher (32 %). The magnetic susceptibility decreases strongly (1-6x10^{-5}SI).

Unit D3 consists of a grey fine sand deposit. The organic content is low (2 %). The carbonate content is similar the previous unit (31 %). The magnetic susceptibility is low (1x10^{-5}SI).

Unit D4 consists of grey clayey-silty sediments. A rolled ceramic has been found at the base. A plant stem has been dated from 1410 to 1464 CE. The organic content is higher (3.5 %). The carbonate content is still high (31 %). The magnetic susceptibility increases again (2-10x10^{-5}SI).

Unit E (1.24 m a.s.l.-0.03 m b.s.l.) consists of yellow–brown silt with a well sorted fine sand. The organic content is low (1–2.5 %). The carbonate content decreases (13 %) and then increases again (25 %).

Unit F (1.24–1.81 m a.s.l.) is a sand-dominated well sorted layer with rare shell fragments. The organic content is low (1–2 %). The carbonate

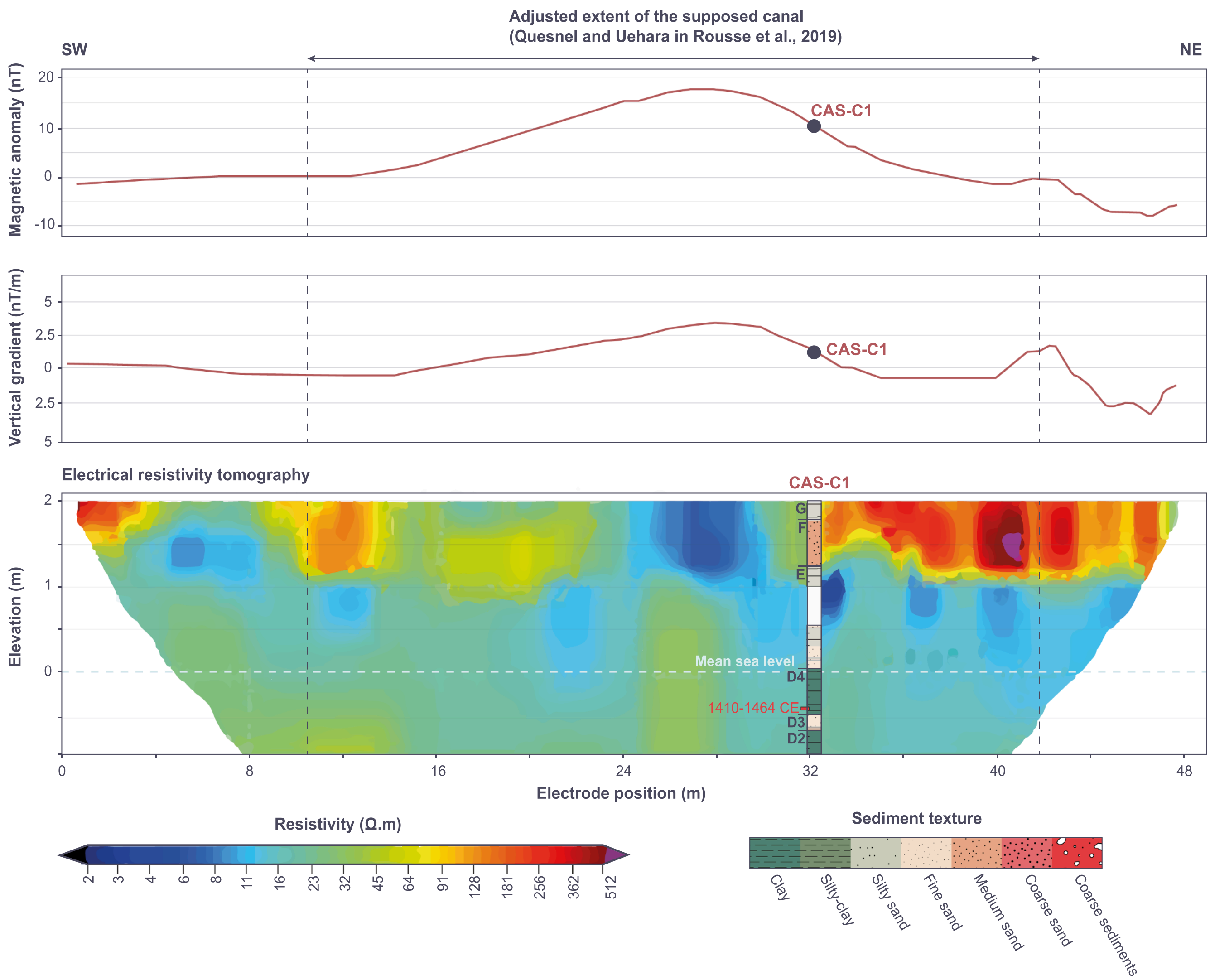

Fig. 4. Core CAS-C1 on the geophysical survey data.

content decreases (30–22 %). The magnetic susceptibility is still low (4x10^{-5}SI).

Unit G (1.81–2.08 m a.s.l.) is composed of yellow–brown silt. The magnetic susceptibility is still low (4x10^{-5}SI).

4.2. Outside of the hypothesised canal (Zone 1) – CAS-C3

CAS-C3 consists of five main units (Fig. 5).

Unit A (7.35–7.45 m b.s.l.) is characterised by dark grey gravels and sands with shell fragments. The organic content is very low (0.5–1 %). The carbonate content is relatively low (4 %). The magnetic susceptibility is low (0.5x10^{-5}SI).

Unit B (4.96–7.35 m b.s.l.) comprises dark grey fine sand and very fine sand with shell hash and two thin layers of rounded pebbles. The organic content is still low (3.7 %). The carbonate content decreases slightly (7.5–6 %). The magnetic susceptibility increases slightly (1x10^{-5}SI).

Unit C1 (3.50–4.96 m b.s.l.) consists of grey to dark grey laminated silts and clays with varying amounts of sand. A piece of wood has been dated from 5201 to 4837 BCE and a plant material has been dated from 4781 to 4750 BCE. *Loripes orbiculatus*, *Parvicardium scriptum*, *Diplodonta*. *intermedia*, *Bornia sebetia*, *Lentidium*.
mediterraneum and *Cerastoderma glaucum* are present (Table 3). The organic content is still low (4 %). The carbonate content remains moderate (6–10 %). The magnetic susceptibility is variable (0.5-6x10^{-5}SI).

Unit C2 (2.86–3.50 m b.s.l.) is composed of grey silts with fine sand. *Bornia sebetia* is present. The organic content is still the same (4 %). The carbonate content remains low (5–9 %). The magnetic susceptibility increases to the top (2-9x10^{-5}SI).

Unit C3 (0.48–2.86 m b.s.l.) is composed of grey silty clay with sands. Plant material found in a silty layer is dated from 1412 to 1197 BCE. *Loripes orbiculatus* is present. The organic content is constant (4–6 %) with a high peak (12 %). The carbonate content is low (7 %). The magnetic susceptibility is stable (1x10^{-5}SI) with an increase towards the top (6x10^{-5}SI).

Unit D (0.94 m a.s.l.-0.48 m b.s.l.) consists of yellow silty clay layers. The organic content is constant (4 %). The carbonate content is decreasing (7.5–5 %). The magnetic susceptibility remains relatively stable (0.5–10 x10^{-5}SI).

Unit E (1.55–0.94 m a.s.l.) consist of well-sorted fine sands. The organic content is low (4 %). The carbonate content is low (5 %). The magnetic susceptibility remains relatively stable (5-8x10^{-5}SI).

4.3. Hypothesised canal (Zone 2) – CAS-C2

The Core CAS-C2 is composed of five stratigraphic units (Fig. 6).

The basal Unit A (6.38–6.53 m b.s.l.) is composed of dark grey coarse

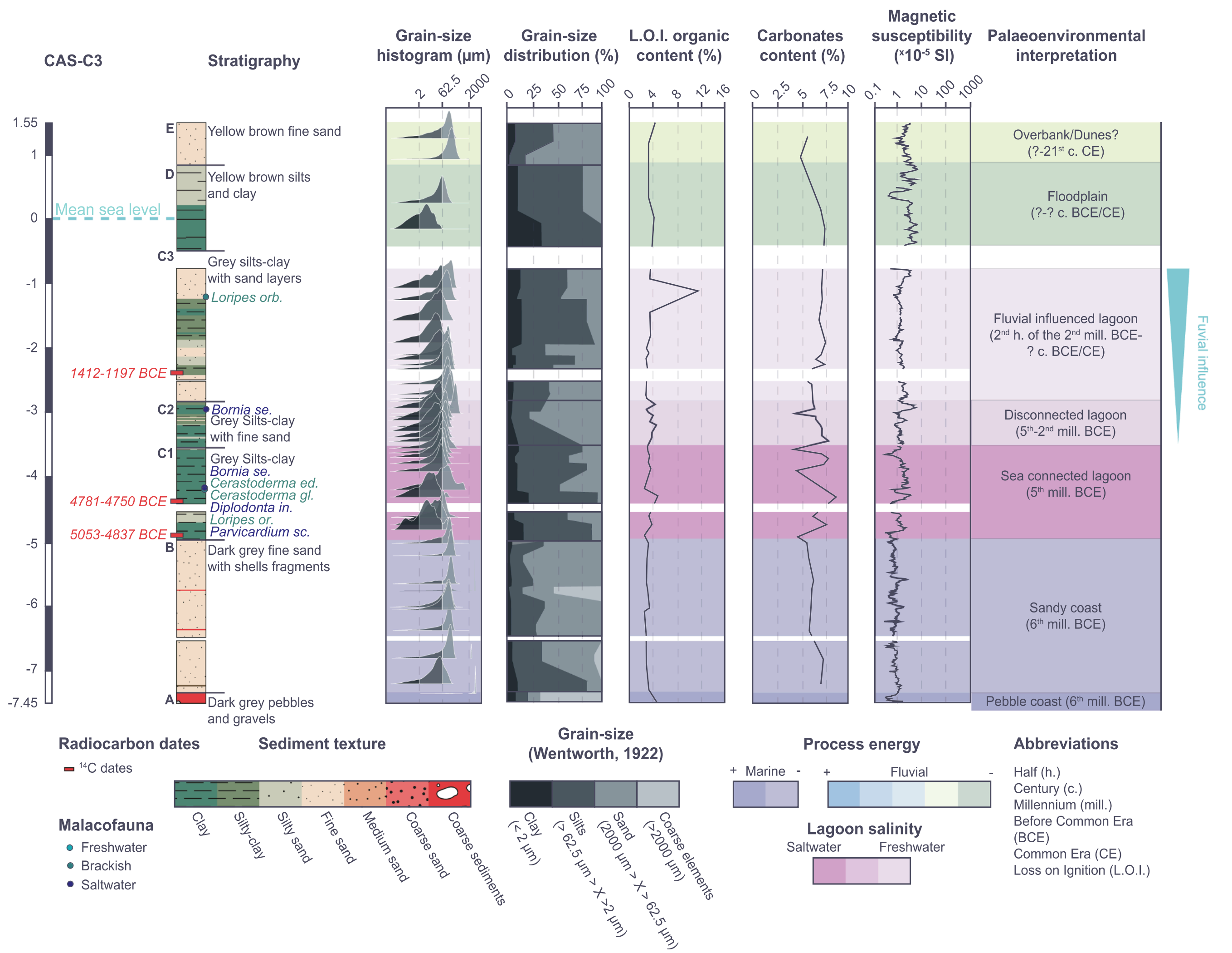

Fig. 5. Palaeoenvironmental diagram of CAS-C3. (See above-mentioned reference for further information.)

elements with shell fragments. Magnetic susceptibility is low (1x10^{-5}SI).

Unit B (5.32–6.53 m b.s.l.) is characterised by the presence of well-sorted laminated fine sands containing shell fragments. Three pieces of wood were respectively dated from 5620 to 5481 BCE and from 5474 to 5309 BCE. Magnetic susceptibility fluctuates slightly (1-5x10^{-5}SI).

Unit C (4.87–5.32 m b.s.l.) is defined by a grey silty clay layer. The magnetic susceptibility increases slightly (5x10^{-5}SI).

Unit D1 (4.48–4.87 m b.s.l.) is characterised by a grey medium sand layer. A piece of wood has been dated trom 540 to 386 BCE. The magnetic susceptibility varies strongly (0.9-10x10^{-5}SI).

Unit D2 (4.11–4.48 m b.s.l.) is composed of grey silts. Magnetic susceptibility values decrease strongly (10-1x10^{-5}SI).

Unit D3 (3.23–4.11 m b.s.l.) is characterised by an alternation of grey medium sands and silts. Magnetic susceptibility varies strongly (0.8-10x10^{-5}SI).

Unit E1 (2.06–3.23 m b.s.l.) is composed of fine grey silty clay. Magnetic susceptibility varies strongly (13x10^{-5}SI).

Unit E2 (0.25–2.06 m b.s.l.) is composed of fine grey silty clay. A piece of plant has been dated from 1876 to 1629 BCE. The magnetic susceptibility has a lower intensity (7x10^{-5}SI).

Unit F (1.47 a.s.l.-0.25 m b.s.l.) is a silty brown layer. A trapped plant stem has been dated from 1032 to 1203 CE. The magnetic susceptibility is slightly variable (7-9x10^{-5}).

5. Discussion

5.1. Transgressive coast

Each collected core revealed the presence of a dark unit consisting mainly of rounded coarse pebbles accompanied by a high density of shell debris (Units A in CAS-C1, C2 and C3) including a *Cerastoderma edule*, a highly adaptable marine species, which may be indicative of conditions associated with the infralittoral zone. These facies showing strong hydrodynamic activity during the 6th mill. BCE which could be explained by the early Holocene transgression which could have promoted waves to rework the Pleistocene formations of the Crau Plain. Marine erosion process caused by waves heavily reworked these coarse materials forming transgressive deposits (Vella et al., 2005). This trend is confirmed by the date at the base of CAS-C1 (Fig. 2). The observed differences in depth can likely be attributed to the irregular topography of the underlying Durancian material, as noted by Provansal et al. (1999; 2003). For instance, Core BSS002JEYH (Fig. 2) records Pleistocene Crau gravels at a depth of 11 m, located just 200 m south of Zone 1. This finding not only emphasises the role of marine erosion in redistributing sediments, but also highlights the influence of the underlying geological formations on Holocene sedimentary deposits. The well-sorted fine sands deposited above are contemporaneous with materials dated to the 6th millennium BCE (Unit B in CAS-C2). The dates obtained for this homogenous body of sand suggest that this is also deposited during the

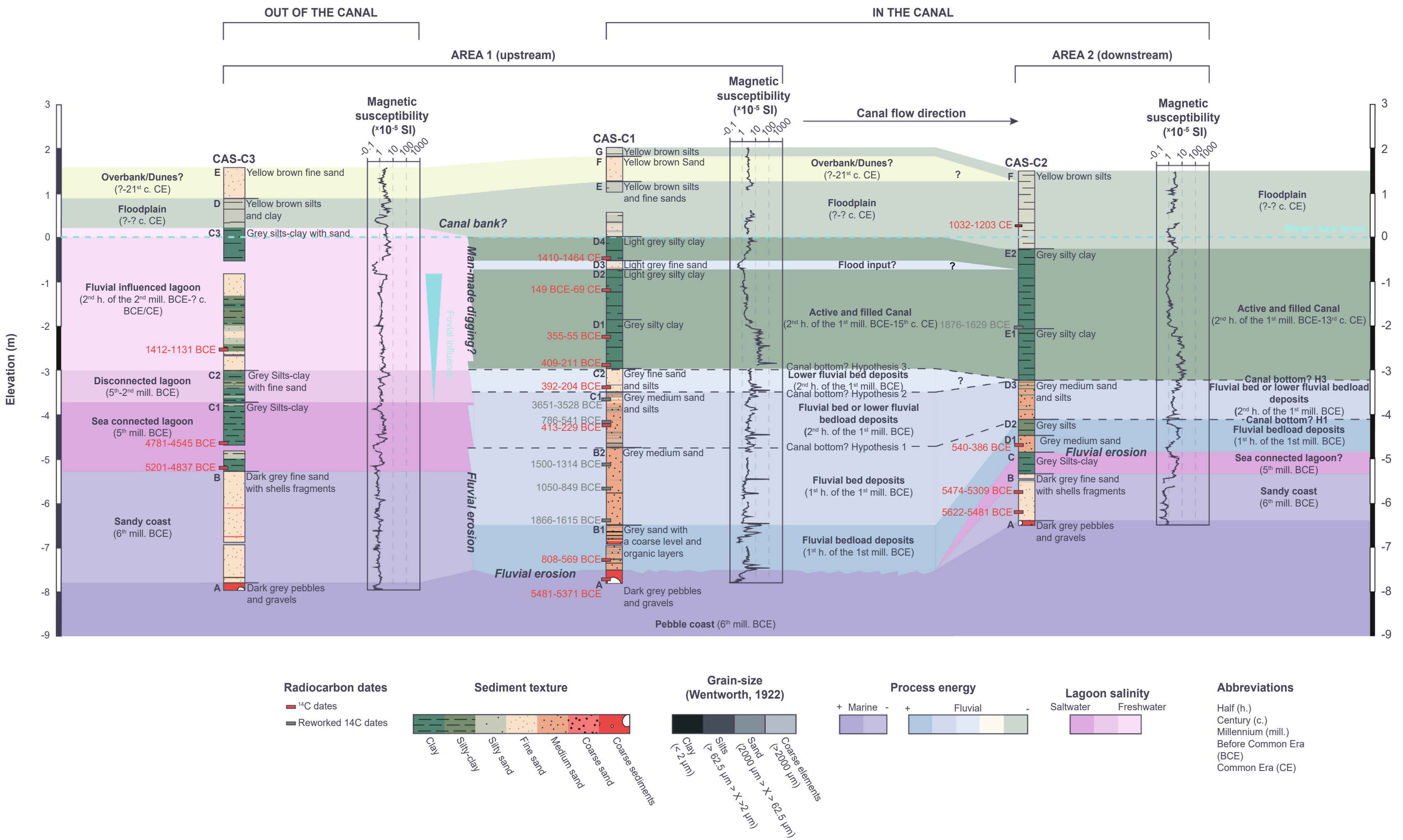

Fig. 6. Summary of the cores drilled in and out of the supposed Marius Canal.

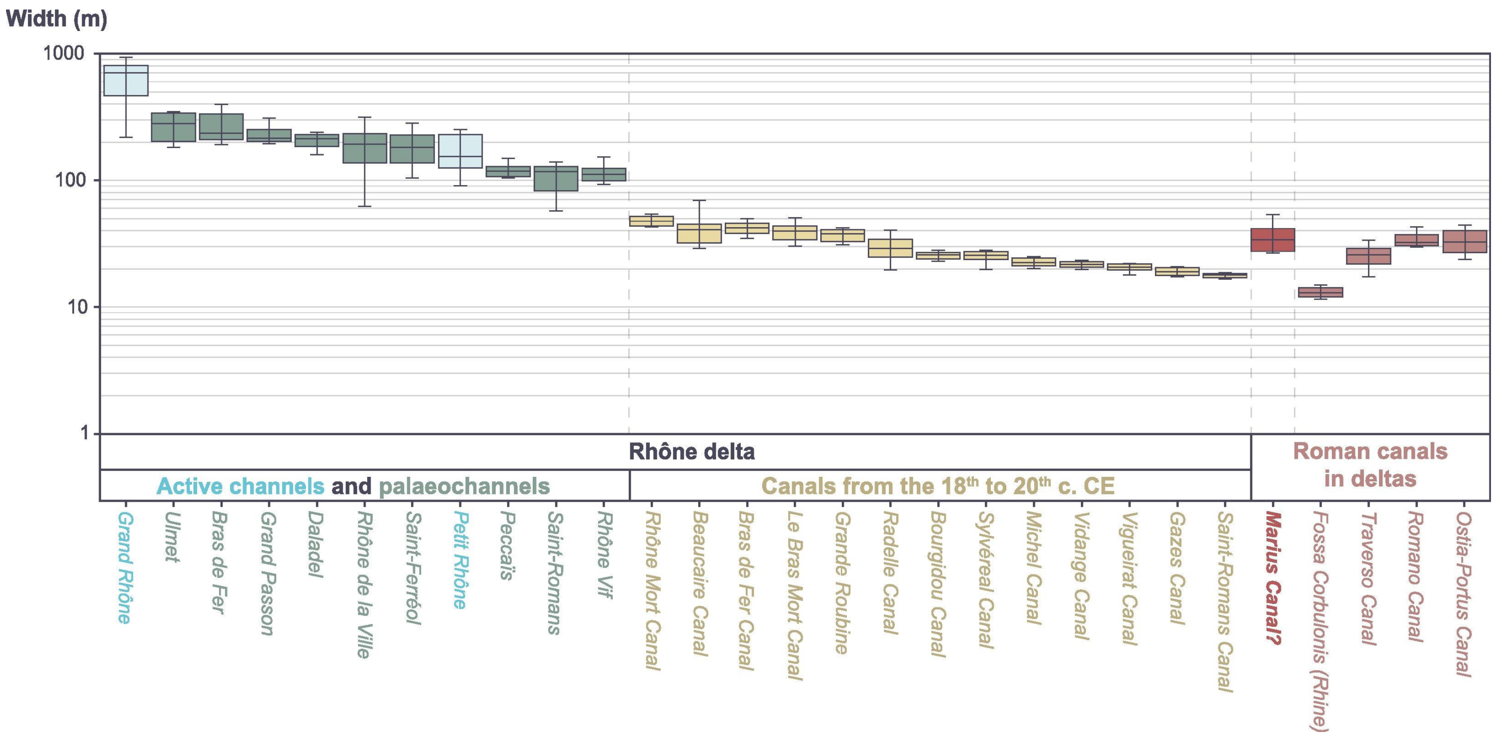

Fig. 7. Width comparison of the presumed Marius canal with the active canals of the Rhône, the palaeochannels, the modern canals and the other Roman deltaic canals.

transgressive period preceding the initiation of the progradation of the Rhône Delta.

5.2. Lagoon setting post-eustatic sea level deceleration

The sediments overlying the earlier marine deposits are clearly different, showing a marked reduction in hydrodynamic activity. The assemblage of species observed at −4.16 m b.s.l. with *Lentidium mediterraneum* is typical of the infralittoral zone (Unit C1 in Core CAS-C3). The additional presence of *Bornia sebetia*, *Cerastoderma glaucum* and *Parvicardium scriptum* also indicates the existence of muddy sediments in calm waters with fluctuating salinity, and therefore a great ecological diversity leading to the development of a wide variety of benthic species. The succession of silty and sandy sediments associated with this malacofauna (Table 3), belonging to euryhaline and euryhaline waters, suggests a lagoonal environment (Nichols and Allen, 1981). While the delta expanded mainly by north–south progradation, an eastern lagoon developed along the Crau Plain, where sediment in mostly stagnant water could accumulate behind a lateral system of coastal barriers (Vella et al., 2005). In the middle (Unit C2 in CAS-C3) and upper (Unit C3 in CAS-C3) sedimentary layers, the gradual absence of shells, an increase in sandy inputs and an increase in organic matter indicate an increased fluvial influence, suggesting a marshy environment with flood input, more sheltered from marine influence (Sanjaume et al., 1992). However, the continuity of a brackish influenced habitat is still attested by *Loripes orbiculatus* at 2.96 m b.s.l. and *Bornia sebetia* at 1.20 m b.s.l. The final filling may have occurred rapidly due to an increase in sediment load from the river feeding the lagoon during the second half of the 2nd mill. BCE and later.

Table 4

Main characteristics of Roman shipwrecks, such as estimated age (BCE/CE), approximate draught and load capacity, classified by size, with references from archaeological research.

Name	Age (BCE/CE)	Draught (m)	Deadweight tonnage (t)	Reference
Small-size vessels				
Cavalière	1st quarter of the 1st c. BCE	≈ 1.15	≈ 22.17	Charlin et al., 1978
Laurons 2	End of the 2nd c. CE	≈ 1.20	≈ 28.35	Gassend, 1984
Arles-Rhône 13	3rd-4th c. CE	≈ 1.70–1.80	≈ 40	Long and Duperron, 2014
Fiumiccino 1	4th-5th c. CE	≈ 1.40	≈ 50	Boetto, 2010
Medium-size vessels				
Saint-Gervais 3	Middle of the 2nd c. CE	≈ 2.36	≈ 81.11	Liou et al., 1990
Bourse de Marseille	160–220 CE	≈ 2.20–2.30	≈ 142	Gassend, 1982
Large-size vessels				
Madrague de Giens	75–60 BCE	≈ 3.75	≈ 402.5	Pomey, 1982

5.3. Eastern Rhône delta palaeochannel in the 1st millennium BCE

The significant variations in grain size observed in the lower stratigraphic unit (Unit B1 in CAS-C1) are probably the result of rapid changes of the hydrological regime within a fluvial channel, occurring on seasonal or annual scales. During floods, coarse and sandy sediments were transported and deposited, while the presence of finer grain sizes points to periods of reduced water flow. This facies exhibits characteristics similar to bedload deposits seen in the Grand Rhône channel, as described by Arnaud-Fassetta et al. (2003). The most recent date obtained from these bedload-derived facies deposits indicates that a channel of the Rhône in this area dates back to the first half of the 1st mill. BCE. This new branch of the Rhône River began to erode the underlying marine deposits in CAS-C1 and partially in CAS-C2. In CAS-C3, the increase in fluvial input is estimated to have occurred earlier, around the second half of the 2nd mill. BCE while the branch was getting closer to the east. Older material inclusions are found in the subsequent thick sandy deposit in CAS-C1 (Unit B2), indicating a period of riverbed aggradation during the 1st mill. BCE, probably due to sediment reworking in the riverbed. Other sediment from an active riverbed could be observed downstream in CAS-C2 (Units D1 and D2). This evidence of a river branch is situated at a minimum distance of 4 km from Ulmet, the nearest documented channel of that time (Fig. 1; Vella et al., 2016). These deposits highlight the presence of an additional distributary, which may represent a palaeo-Grand Rhône. This would have formed an additional channel in ancient times, contributing to the gradual fluvial expansion observed between the end of the 2nd mill. BCE and at least the 1st c. BCE (Arnaud-Fassetta et al., 2000; Excoffon et al., 2004; Berger and Bravard, 2012).

5.4. An operational canal during the Roman period

First of all, the magnetic signature detected by surface magnetic survey seems to coincide with the high magnetic susceptibility response measured between 2 and 3.5 m b.s.l. (Fig. 3.; Unit D1 in CAS-C1; Unit E1 in CAS-C2). Although the cause of this phenomenon remains unclear, this magnetic signature allows us to link the stratigraphic results to the surface magnetic anomaly and supports the existence of a long and narrow palaeochannel (Fig. 4). These two units in CAS-C1 and C2 are grey silty clay of fluvial origin. This linear feature could be associated with these fluvial sediments, leading to the palaeochannel hypothesis. In terms of geometry, the low degree of sinuosity is generally synonymous with human intervention and therefore of a questionable 'naturalness'. This type of straight morphology could be observed in rare cases in very steep systems such as torrents (Malavoi and Bravard, 2010), but not in lowland areas prone to meandering channels. It's narrowness (no more than 30 m wide) makes it unlikely to be a natural distributary, as these are generally much wider (Fig. 7). For comparison, near Portus the Tiber River is 110 to 180 m wide (today) and Roman canals were 25 m (Canale di Comunicazione Traverso), 35 m (Canale Romano), and 25 to 40 m wide (Northern Canal and Portus-to-Ostia Canal – not considering lateral mobility) (Salomon et al., 2016). The geometry is consistent with an anthropogenic origin, sufficiently wide to accommodate large ships.

In order to estimate the maximum draught of ships that could have utilised the canal, the draughts of Roman shipwrecks were examined in conjunction with the canal depths and the modelled mean sea level curve (Salomon et al., 2016). It must be acknowledged, however, that accurately assessing tonnage remains a challenging endeavour (Pomey and Tchernia, 1978; Pomey and Rieth, 2005; Nantet, 2014), and that the ensuing interpretations will be based on an order of scale. The shipwrecks selected are dated Roman vessels, the draughts of which have been estimated using a graphical method, and the age indicated corresponds to the terminus post quem of the goods or the vessel (Table 4).

Regarding the canal bottom, three hypotheses are possible. The first one (Hypothesis 1 in Figs. 3, 6 and 7) shows an alternation of fine and coarse sediments and could be related to a channel bedload similar to the palaeo-Rhodanian channel but without pebbles. Unfortunately, the date obtained does not match with the Marius hypothesis (Group 1 in Fig. 8). The second hypothesis (Hypothesis 2 in Figs. 3, 6 and 8) is a sandy layer different from the underlying sands since it has a good sorting index and carbonate content equivalent to the fine sediments above. In addition, two fluvial species with moderate tolerance to salt water were identified in these levels (Fig. 2). This particular deposit could be explained by the fact that the junction where the canal diverts the Rhône could be in a section where only a certain fraction of sediment enters the canal. Nevertheless, this unit is absent in the CAS-C2 core downstream and the associated date is also from the 2nd half of the 1st mill. BCE (Group 2 in Fig. 8). The two initial hypotheses may also be fluvial deposits transported by the palaeo-Grand Rhône described in the previous section. The last possible bottom could be Unit D1 (Hypothesis 3 in in Figs. 3, 6 and 8). The deposits would be associated with slow flow rate allowing only fine sediments to be transported. In that case, the upstream of the canal should have been managed using specific structures like locks.

In the lower part of this canal, there is no contemporary date with the Marius Canal excavation event (Group 2 in Fig. 6) but the filling sediments above contains two dates covering the 1st c. BCE (Group 3 in Fig. 6). When canals are dug and connected to the natural river, the channel adapts to the hydro-sedimentary conditions of the connected river. This adaptation takes place through a number of interacting processes (variations in flow velocity, changes in the longitudinal profile of the river, etc.), leading to equilibrium periods of varying length depending on the main channel. These events are strong transporters of sediments and could explain these floor deposits with older materials. The presence of these dates in the canal is the result of the collapse of river banks, which can occur in the absence of solid structures such as masonry or cement. In the Rhône Delta, local actors involved in the canal system management have identified the main challenge associated with maintaining the canals as being the frequent collapse of the banks (Parc Naturel Régional de Camargue, 2017). Banks are the primary source of sediment for active channels, and their stability is weakened by fauna (e.g. holes), as well as by the accumulation of fallen trees, leading to the widening and filling in of the canals over time (ibid). Dated stakes from the Roman period found nearby may be evidence of the latest adjustments in response to this recurrent phenomenon.

For any of the three hypotheses, the water column was deemed to be appropriate for a medium vessel size or smaller (Fig. 8). The presence of

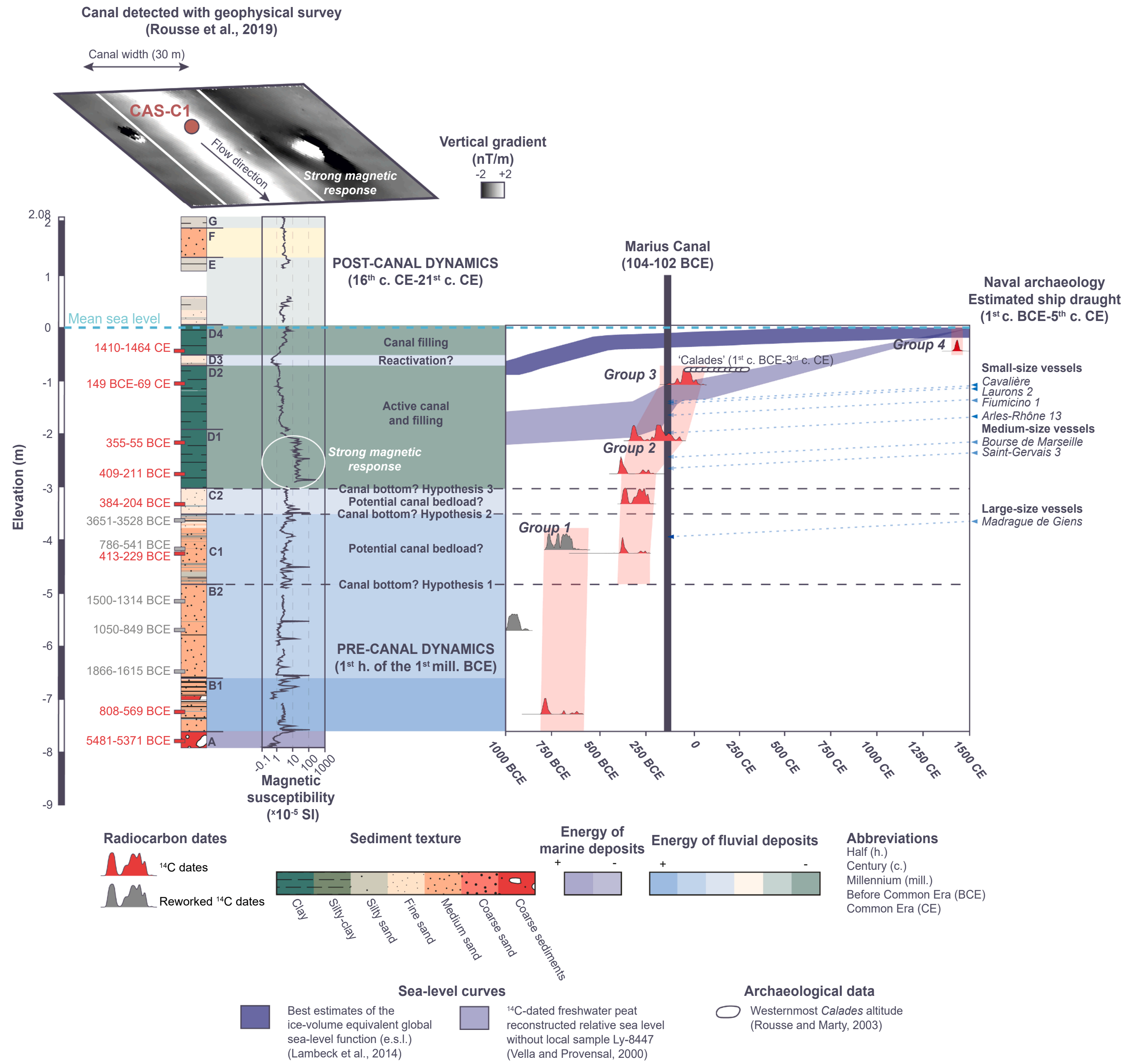

Fig. 8. Synthesis of geoarchaeological knowledge of the supposed Marius Canal.

Stake 2 (131–326 CE) may be indicative of potential activity along the canal until the first quarter of the 4th c. CE. The lowest point of a navigable canal related to this stake would be characterised by a depth of less than with fine deposits one metre. Only vessels with a flat bottom would have been able to navigate.

The filling of the canal with fine deposits is either an evidence of its quick abandonment or a slow abandonment. The clay fill shows strong similarities to a sequence of either an avulsion or a meander cut that does not induce flood channel migration (Cojan and Renard, 2006). This process resulted in a reduction in hydrological power, leading to rapid sedimentation processes and the formation of lentic facies (Slingerland and Smith, 2004). This type has also been observed in other Roman canal cases, such as the Fossa Corbulonis, excavated around 47 CE (de Kort and Raczynski-Henk, 2014). A subsequent temporary hydrological reconnection to the Rhône is recorded by the presence of a fine sand input but the canal is totally filled by the 15th c. CE in zone 1 (group 4 in Fig. 8). The existence of this canal should be interpreted in the context of the development of the port of Fos and in close connection with the recent discovery of the Roman site on its southern bank. (Rousse and Marty, 2023).

5.5. Post-canal dynamics

Post-canal dynamics correspond to fine sediment floodplain deposits dated to the end of the Middle Ages during periods of important floodplain or swamp cover (Stouff, 1993). The well-sorted fine sands deposited in a terrestrial context may be indicative of either overbank deposits or local wind deposits, termed *montilles* (Arnaud-Fassetta and Provansal, 1993). These deposits may be mistaken for overbank deposits and whose particles are derived either from former beach-ridges or ancient alluvial deposits (Arnaud-Fassetta and Provansal, 1993). In the Modern period (16th-19th c. CE), examination of paleochannel logs has exposed

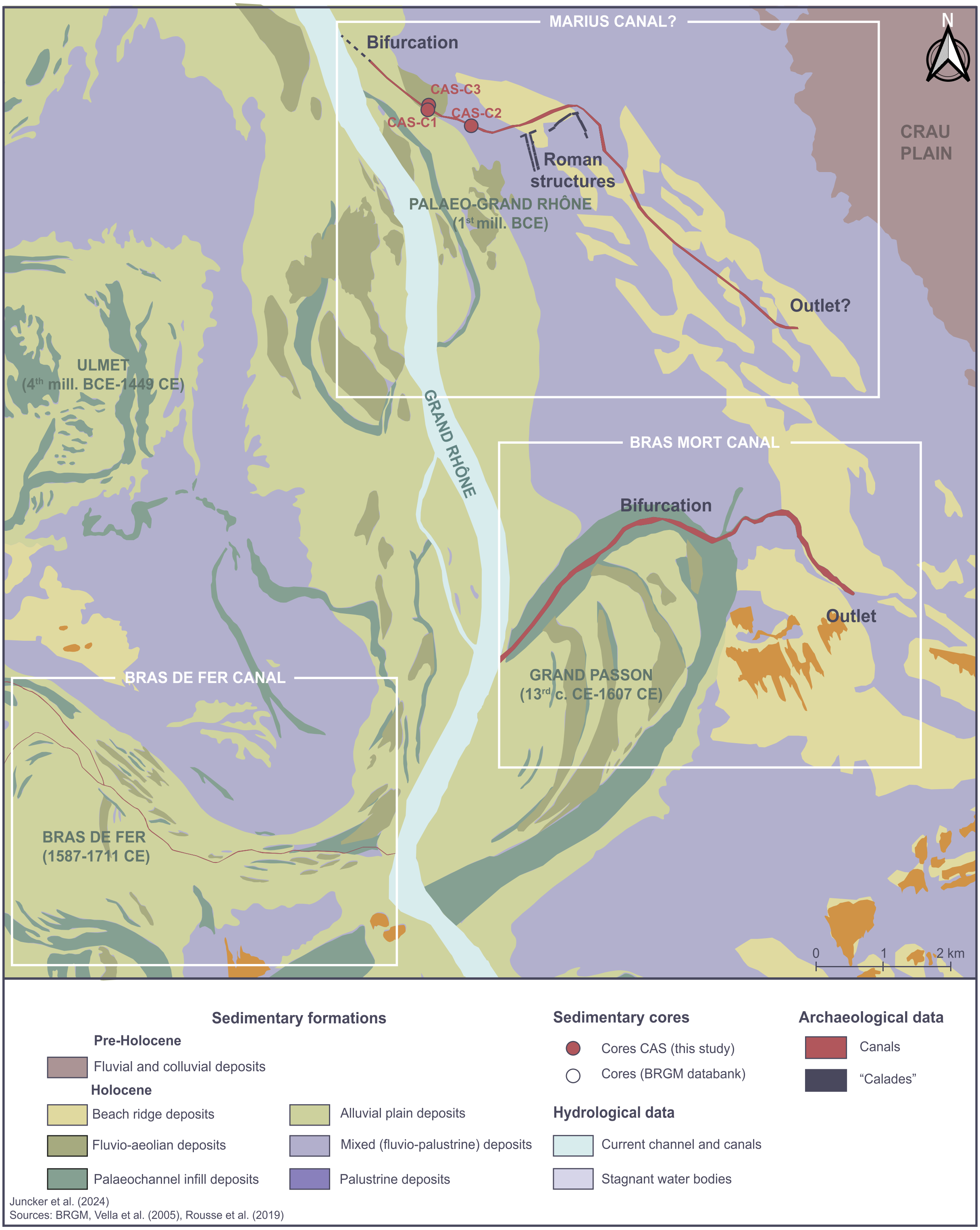

Fig. 9. Patterns of canal connections in the eastern part of the Rhône Delta.

significant fluvial mobility (Fig. 1) and phases of major floods are well documented at the end of the 16th c. and the beginning of the 18th c. (Rey, 2010; Pichard et al., 2014).

5.6. *Cross-period lessons on canal excavations strategies in the Rhône delta*

Examples of modern canals constructed under similar conditions can enhance our understanding of the supposed Marius Canal. A particularly relevant example can be found south of the Vigueirat Marshes, where the Rhône River formed the Grand Passon, a large meander that was active from the 13th c. CE until 1607 CE (Fig. 1). This paleochannel was later repurposed for the construction of the Canal du Bras Mort (Fig. 9). The canal flows southeast into the Galéjon Pond near Fos-sur-Mer, establishing a connection between Fos-sur-Mer and the Rhône during the Modern period (16th-19th c. CE). A similar example exists on the right bank of the Rhône: the Bras de Fer Canal, which follows the course of the Bras de Fer paleochannel, was used for navigation at least during the 16th c. CE (Rambert, 1993). Unlike the straight alignment of the Arles-Bouc Canal, the course of the presumed Marius Canal appears to follow a paleochannel for it's upstream reach and then towards marshy areas, like modern examples. In the case of the Marius Canal, its route is explained by the military urgency of the situation, completed by legionaries in just two years. Roman engineers likely sought to expedite construction by targeting areas that could be excavated quickly, such as existing channels or marshlands. However, it is important to differentiate between canals built for military purposes and those developed for economic purposes in later periods (Salomon and Rousse, 2023). A specific element of the Fossa Marianae is its evolution from military infrastructure to a main commercial waterway. This transformation may reflect later adaptations of the canal for new purposes, possibly including the addition of supplementary canals to improve connectivity. This shift in function might explain the transition from hydronym to toponym in ancient sources when referring to the port station, e.g. Fossae Marianae (Rousse et al., 2019).

6. Conclusion

The present study offers significant insights into a new hypothesis for the Marius Canal, its functionality and its development, particularly addressing the complexities in accurately dating such structures. The combination of multi-proxy sediment core analyses and previous geophysical data supports the hypothesis of a Roman navigable canal associated with the linear feature identified by Badan (2013). It also highlights the importance of an integrated geoarchaeological and archaeological approach in studying ancient canal systems. Evidence of this canal, dug in a natural palaeochannel, is often amalgamated with prior sediments, complicating their chronological assessment. However, the canal's notable dimensions and archaeological evidence align strongly with a Roman origin. Some uncertainties persist, including the precise depth of the canal, its hydraulic connections with the Rhône and the Mediterranean, and the presence of related structures like quays or towpaths. Further archaeological research would be essential to confirm or refute whether this canal can be attributed to the troops of Consul Gaius Marius, but it is clear that this Roman canal was an essential part of the Arles-Fos port system.

CRediT authorship contribution statement

Joé Juncker: Writing – original draft, Visualization, Methodology, Investigation, Conceptualization. **Ferréol Salomon:** Writing – original draft, Supervision, Resources, Methodology, Investigation, Conceptualization. **Corinne Rousse:** Writing – original draft, Supervision, Resources, Project administration, Methodology, Investigation, Funding acquisition, Conceptualization. **Grzegorz Skupinski:** Writing – review & editing, Investigation. **Yoann Quesnel:** Writing – review & editing, Resources. **Minoru Uehara:** Writing – review & editing, Resources. **Iscia Codjo:** Writing – review & editing, Investigation. **Nicolas Carayon:** Writing – review & editing, Investigation. **Benoît Devillers:** Writing – review & editing, Resources. **Claude Vella:** Writing – review & editing, Resources, Conceptualization.

Funding

We are grateful to the Fos-Ostie-Portus: Harbours of Roman Antiquity – Fosphora project (2019–2021) for their support in making this publication possible. We would also like to acknowledge the Excellence Initiative of Aix-Marseille Université – A*MIDEX, a French "Investissements d'Avenir" programme, AMX-18-MED-018, for their contribution to the project.

Declaration of competing interest

The authors declare that they have no known competing financial interests or personal relationships that could have appeared to influence the work reported in this paper.

Acknowledgements

We would like to express our gratitude to Marie-Brigitte Carre and Catherine Virlouvet, the project coordinators of the Fosphora project, as well as all the members of the project. we would like to thank the Service Régional de l'Archéologie Provence-Alpes-Côte d'Azur for their financial support. We would also like to acknowledge the assistance provided by Jean-Laurent Lucchesi, Leïla Debiesse, Christophe Pin, Clément Pappalardo and Morad Balti from the Association Les Amis des Marais du Vigueirat for kindly assisting us in accessing the site and for their invaluable help with drilling. We would also like to express our gratitude to Othello Badan and Mario Maretti for their invaluable assistance and for the stimulating discussions we had together. Finally, we are also grateful to Martine Trautmann and Sylvain Bernarioumlil from the Laboratoire des Sols et des formations superficielles for their expertise.

Data availability

Data will be made available on request.

References

Ambert, P., 2000. Narbonne antique et ses ports, géomorphologie et archéologie, certitudes et hypothèses. Revue Archéologique De Narbonnaise 33, 295–307.

Ambert, P., 1998. Le cadre géographique et géologique de Narbonne antique. 120ème congrès national des Sociétés savantes historiques et scientifiques Aix-en-Provence 1995, 93-106.

Arnaud, P., 2005. Les routes de la navigation antique: itinéraires en Méditerranée, Paris, Editions Errance.

Arnaud-Fassetta, G., 1998. Dynamiques fluviales holocènes dans le delta du Rhône. University Aix-Marseille I. PhD Thesis.

Arnaud-Fassetta, G., Landuré, C., 1997. Occupation du sol et contraintes fluviales dans le delta du Rhône (France du Sud). In: Burnouf, J., Bravard, J.-P., Chouquer, G. (Eds.), La dynamique des paysages protohistoriques, antiques, médiévaux et modernes, XVIIe Rencontres Internationales d'Archéologie et d'Histoire d'Antibes. ADPCA, Sophia Antipolis, pp. 285-308.

Arnaud-Fassetta, G., Suc, J.-P., 2015. Dynamique hydrogéomorphologique et diversité végétale dans le delta du Rhône (France) de -10 000 ans à demain. In: Reynard, E., Evéquoz-Dayen, M., and Borel, G. (Eds.), Le Rhône, entre nature et société. Cahiers de Vallesia, 29, Sion, pp. 63-98.

Arnaud-Fassetta, G., Provansal, M., 1993. Étude géomorphologique du delta du Rhône : l'évolution des milieux de sédimentation fluviatiles au cours de l'Holocène récent. Méditerranée 78 (3–4), 31–42. https://doi.org/10.3406/medit.1993.2833.

Arnaud-Fassetta, G., De Beaulieu, J.-L., Suc, J.-P., Provansal, M., Williamson, D., Leveau, P., Aloïsi, J.-C., Gadel, F., Giressè, P., Oberlin, C., Duzer, D., 2000. Evidence for an early land use in the Rhone delta (Mediterranean France) as recorded by late Holocene fluvial paleoenvironments (1640-100 BC). Geodin. Acta 13, 377–389. https://doi.org/10.1080/09853111.2000.11105381.

Arnaud-Fassetta, G., Quisserne, D., Antonelli, C., 2003. Downstream grain-size distribution of surficial bed material and its hydro-geomorphological significance in a large and regulated river: the Rhône River in its delta area (France) / Distribution granulométrique longitudinale des dépôts de fond superficiels et sa signification hydro-géomorphologique dans un grand fleuve chenalisé : le Rhône dans son aire deltaïque (France). Géomorphologie : Relief, Processus, Environnement 9, 33–49. https://doi.org/10.3406/morfo.2003.1164.

Arnaud-Fassetta, G., Bruneton, H., Berger, J.-F., Beaudouin, B., Boes, X., Provansal, M., 2005. A ~ 8000-yr record of palaeohydrology and environmental change in fluvial-influenced sediments from Arles-Piton core, upper Rhône Delta France. Zeitschrift Für Geomorphologie 49 (4), 455–484.

Arnaud-Fassetta, G., Provansal, M., 2014. The Lower Valley and the Delta of the Rhône River: Water Landscapes of Nature and History. In: Fort, M., André, M.-.-F. (Eds.), Landscapes and Landforms of France, World Geomorphological Landscapes. Springer, Netherlands, Dordrecht, pp. 207–218. https://doi.org/10.1007/978-94-007-7022-5_20.

Badan, O., 2013. Sur les traces du canal de Marius. Bulletin Des Amis Du Vieil Arles 158, 27–28.

Ball, D.F., 1964. Loss-on-ignition as an estimate of organic matter and organic carbon in non-calcareous soils. J. Soil Sci. 15 (1), 84–92. https://doi.org/10.1111/j.1365-2389.1964.tb00247.x.

Bellan-santini, D., Lacaze, J.-C., Poizat, C., 1994. *Les biocénoses marines et littorales de Méditerranée*. Collection Patrimoines Naturels.

Benoît, F., 1964. Le développement de la colonie d'Arles et la centuriation de la Crau. Comptes Rendus Des Séances De L'académie Des Inscriptions et Des Belles-Lettres 108–1, 156–169. https://doi.org/10.3406/crai.1964.11706.
Benoît, F., 1936. Forma Orbis Romani. Carte (partie occidentale) et texte complet du département des Bouches du Rhône. Carte archéologique de la Gaule romaine, 5, Paris, Ernest Leroux, 232.
Berger, J.-F., Bravard, J.-P., 2012. Le développement économique romaine face à la crise environnementale : le cas de la Gaule narbonnaise. In: Berger, J.-.-F. (Ed.), Des Climats et Des Hommes. Éditions La Découverte, Paris, pp. 269–288.
Boetto, G., 2010. Le port vu de la mer : l'apport de l'archéologie navale à l'étude des ports antiques. Bolletino di Archeologia Online, vol. Special issue: XVII[th] International Congress of Classical Archaeology, Roma 22-26 Septembre 2008, 112-128.
Brousse, G., Arnaud-Fassetta, G., 2011. Caractérisation (2010) et évolution récente (1999-2010) du gradient granulométrique longitudinal dans les deux bras du Rhône deltaïque (France méditerranéenne). Géomorphologie 17, 291–306. https://doi.org/10.4000/geomorphologie.9500.
Bruneton, H., Arnaud-Fassetta, G., Provansal, M., Sistach, D., 2001. Geomorphological evidence for fluvial change during the Roman period in the lower Rhône valley southern France. Catena 45, 287–312. https://doi.org/10.1016/S0341-8162(01)00143-6.
Charlin, G., Gassend, J.-M., Lequément, R., 1978. L'épave antique de la baie de Cavalière (Le Lavandou, Var). Archaeonautica 2, 9–93. https://doi.org/10.3406/nauti.1978.867.
Clerc, M., 1906. La bataille d'Aix : études critiques sur la campagne de Caius Marius en Provence. Fontemoing, Marseille, Barlatier, Paris.
Cojan, I., Renard, M., 2006. Sédimentologie. Dunod, 2ème edition.
Collin Bouffier, S., 2009. Marseille et la Gaule méditerranéenne avant la conquête romaine. Pallas 35–60. https://doi.org/10.4000/pallas.1751.
Colomb, E., Roux, R.-M., 1978. La Crau, données nouvelles et interprétations. Géologie Méditerranéenne 5, 303–323. https://doi.org/10.3406/geolm.1978.1052.
Colomb, E., Roux, M.R., 1986. La Crau, histoire Plio-Pléistocène. Méditerranée 58, 31–42. https://doi.org/10.3406/medit.1986.2404.
Compatangelo-Soussignan, R., 2016. Poseidonios and the original cause of the migration of the Cimbri : Tsunami, storm surge or tides? Revue Des Études Anciennes 118 (2), 18.
Cossignani, T., Ardovini, R., 2011. Mediterranean malacology. Atlas of Mediterranen seashells.
D'Angelo, G., Gargiullo S., 1978. Guida alle conchiglie mediterranee. Conoscerle, cerarle, collezionarle, Fabbri Editori.
de Izarra, F., 1993. Le fleuve et les hommes en Gaule romaine. Editions Errance, Paris.
de Kort, J.-W., Raczynski-Henk, Y., 2014. The Fossa Corbulonis between the Rhine and Meuse estuaries in the Western Netherlands. Water Hist. 6 (1), 51–71. https://doi.org/10.1007/s12685-014-0097-3.
Dearing, J.A., 1999. Environmental magnetic susceptibility: using the Bartington MS2 system. Chi Pub, Kenilworth.
Demougeot, E., 1965. Variations climatiques et invasions. Presses Universitaires De France 233 (1), 1–22.
Desjardins, E., 1876. Géographie historique et administrative de la Gaule romaine. I. Introduction et géographie physique comparée : époque romaine-époque actuelle. Paris, Hachette.
Djaoui, D., 2017. Les différents ports du delta du Rhône au Haut Empire : modèle économique autour de la circulation et la diffusion des produits. Archaeonautica 123–140. https://doi.org/10.4000/archaeonautica.496.
Donnadieu, A., 1954. La campagne de Marius dans la Gaule Narbonnaise (104-102 av. J.-C). La bataille d'Aix-en-Provence (Aquae Sextiae) et ses deux épisodes. Revue Des Études Anciennes 56, 281–296. https://doi.org/10.3406/rea.1954.3507, 3–4.
Excoffon, P., Landuré, C., Pasqualini, M., 2004. Habitat et risque fluvial dans le delta du Rhône au I[er] siècle av. J.-C., les habitats de la Capelière et du Grand Parc en Camargue. In: Burnouf, J., Leveau, P. (Eds.), Fleuves et marais, une histoire au croisement de la nature et de la culture, sociétés préindustrielles et milieux fluviaux, lacustres et palustres : pratiques sociales et hydrosystèmes. Comité des travaux historiques et scientifiques, Archéologie et histoire de l'art, 19, pp. 85-92.
Faïsse, C., Mathé, V., Bruniaux, G., Labussière, J., Cavero, J., Jézégou, M.-P., Lefèvre, D., Sanchez, C., 2018. Palaeoenvironmental and archaeological records for the reconstruction of the ancient landscape of the Roman harbour of Narbonne (Aude, France). Quat. Int. 463, 124–139. https://doi.org/10.1016/j.quaint.2017.03.072.
Fleming, K., Johnston, P., Zwartz, D., Yokoyama, Y., Lambeck, K., Chappell, J., 1998. Refining the eustatic sea-level curve since the Last Glacial Maximum using far- and intermediate-field sites. Earth Planet. Sci. Lett. 163, 327–342. https://doi.org/10.1016/S0012-821X(98)00198-8.
Fontaine, S., Marty, F., Amouri, M.E., Rousse, C., Borel, L., Carre, M.-B., Carayon, N., Greck, S., Marlier, S., 2019. Le système portuaire du golfe de Fos et le canal de Marius : un état des lieux. Revue Archéologique De Narbonnaise 15–54. https://doi.org/10.3406/ran.2019.1977.
Galloway, W.E., 1975. Process framework for describing the morphologic and stratigraphic evolution of deltaic depositional systems. In: Broussard, M.L. (Ed.), Deltas: Models for Exploration. Houston Geological Society, pp. 87–98.
Gassend, J.-M., Liou, B., Ximénès, S., 1984. L'épave 2 de l'anse des Laurons (Martigues, Bouches-du-Rhône). Archaeonautica 4, 75–105. https://doi.org/10.3406/nauti.1984.953.
Gassend, J.-M., 1982. Le navire Antique du Lacydon. Musée d'Histoire de Marseille.
Grewe, K., 2008. Tunnels and Canals. In: Oleson, J.P. (Ed.), The Oxford Handbook of Engineering and Technology in the Classical World. Oxford University Press, pp. 319–336.
Hoffmann, F., Pellegrin, J.-C., 1997. Une méthode de calcimétrie fine (par dissolution à l'HCl et titration à l'EDTA). Karstologia : Revue De Karstologie et De Spéléologie Physique 30 (1), 55–56. https://doi.org/10.3406/karst.1997.2848.
Hori, K., Saito, Y., 2007. An early Holocene sea-level jump and delta initiation. Geophys. Res. Lett. 34 (L18401), 5. https://doi.org/10.1029/2007GL031029.
L'Homer, A., Bazile, F., Thommeret, J., Thommeret, Y., 1981. Principales étapes de l'édification du delta du Rhône de 7000 BP à nos jours. Océanis 7, 389–408.
Lambeck, K., Rouby, H., Purcell, A., Sun, Y., Sambridge, M., 2014. Sea level and global ice volumes from the Last Glacial Maximum to the Holocene. Earth, Atmospheric, and Planetary Sciences, U.S.A. 111, 15296–15303. https://doi.org/10.1073/pnas.1411762111.
Landuré, C., Dussouillez, P., Fleury, J., Guibal, F., Quesnel, Y., Uehara, M., Vella, C., 2014. Marais du Vigueirat (Camargue, commune d'Arles). Aix-en-Provence, Service Régional d'Archéologie, Provence-Alpes-Côte d'Azur.
Leveau, P., 2004b. La cité romaine d'Arles et le Rhône: La romanisation d'un espace deltaïque. Am. J. Archaeol. 108, 349–375. https://doi.org/10.3764/aja.108.3.349.
Leveau, P., 2014. Le Rhône romain dans sa basse plaine et dans son delta. Variations territoriales, sociétales et environnementales. Revue Archéologique De Narbonnaise 47, 9–34. https://doi.org/10.3406/ran.2014.1896.
Leveau, P., Trousset, P., 2000. Les sources écrites gréco-romaines et l'histoire naturelle des littoraux. Méditerranée 94, 7–14. https://doi.org/10.3406/medit.2000.3148.
Leveau, P., 2004a. Le Rhône et les Romains "terrassiers infatigables, hydrauliciens habiles", la géoarchéologie et le renouvellement d'un paradigme. In: Burnouf, J., Leveau, P. (Eds.), Fleuves et marais, une histoire au croisement de la nature et de la culture, sociétés préindustrielles et milieux fluviaux, lacustres et palustres : pratiques sociales et hydrosystèmes. Comité des travaux historiques et scientifiques, Archéologie et histoire de l'art, 19, pp. 85-92.
Liou, B., Sciallano, M., 1989. Le trafic du port antique de Fos dans l'Antiquité. In: Rivet, L. (Ed.), Actes du congrès de Lezoux. 4-7 mai 1989. Marseille, SFECAG, pp. 153-167.
Liou, B., Gassend, J.-M., Roman, R., 1990. L'épave Saint-Gervais 3 à Fos-sur-Mer (milieu du I[er] siècle ap. J.-C). Archaeonautica 10, 157–264. https://doi.org/10.3406/nauti.1990.906.
Long, L., Duperron, G., 2014. Note préliminaire sur l'épave Arles-Rhône 13, un navire de mer en contexte fluvial à Arles au IV[e] siècle ap. J.-C. Cahiers d'archéologie subaquatique, fouilles et recherches archéologiques en mer, lacs et cours d'eau, XXII, 115-143.
Long, L., Duperron, G., 2016. Navigation et commerce dans le delta du Rhône durant l'Antiquité : bilan des recherches sur le port fluvial d'Arles et ses avant-ports maritimes. In: Sanchez, C., Jézégou, M.-P. (Eds.), Les ports dans l'espace méditerranéen antique : Narbonne et les systèmes portuaires fluvio-lagunaires, actes du colloque international tenu à Montpellier du 22 au 24 mai 2014. Revue Archéologique de Narbonnaise, 44, pp. 199-217.
Lugand, R., 1926. Note sur l'itinéraire maritime de Rome à Arles. Mélanges De L'école Française De Rome 43, 124–139. https://doi.org/10.3406/mefr.1926.8547.
Luginbühl, T., 2014. La migration des Cimbres et des Teutons, une histoire sans archéologie. Archaeol Mosellana 343–360.
Makaske, B., Maas, G.J., van Smeerdijk, D.G., 2008. The age and origin of the Gelderse IJssel. Netherlands J Geosci Geologie En Mijnbouw 87 (4), 323–337. https://doi.org/10.1017/S0016774600023386.
Malavoi, J.-R., Bravard, J.-P., 2010. Éléments d'hydromorphologie fluviale. Office national de l'eau et des milieux aquatiques.
Marlier, S., 2018. Navires et navigations dans le delta du Rhône à l'époque romaine. Archaeonautica 20, 103–140. https://doi.org/10.4000/archaeonautica.528.
Matheron, P., 1825. Plan de Fos et de ses environs, où sont indiqués les emplacements des villes anciennes : Maritima Avaticorum Stomalimne, Fossae Marianae, et les camps retranchés de Marius.
Michez, N., Fourt, M., Aish, A., Bellan, G., Bellan-Santini, D., Chevaldonné, P., Fabri, M.-C., Goujard, A., Harmelin, J.-G., Labrune, C., Pergent, G., Sartoretto, S., Vacelet, J., Verlaque, M., 2014. Typologie des biocénoses benthiques de Méditerranée. Version 2, Rapport du Service du Patrimoine Naturel, Muséum d'Histoire Naturelle, Paris.
Nantet, E., 2014. Combien pouvait-il transporter ? Mesurer le tonnage d'un navire n'est pas une simple affaire. Dialogues D'histoire Ancienne 12, 201–210. https://doi.org/10.3917/dha.hs93.0201.
Nichols, M., Allen, G., 1981. Sedimentary processes in coastal lagoons. In: Coastal lagoon research, present and future, proceedings of an Unesco/IABO seminar. Unesco technical papers in marine science, 33, pp. 27-80.
Oomkens, E., 1970. Depositional sequences and Sand distribution in the postglacial Rhône delta complex. In: Morgan, J.P., Shaver, R.H. (Eds.), Deltaic Sedimentation Modern and Ancient. SEPM Society for Sedimentary Geology, special publication, 15, 198-212.
Pérès, J.-M., Picard, J., 1964. Nouveau manuel de bionomie benthique de la mer Méditerranée. Édition Revue et Augmentée, Recueil Des Travaux De La Station Marine D'endoume 31 (47), 1–137.
Peter, P., 2021. Archéologie et Histoire des canaux de navigation en France métropolitaine (II[e] s. av. J.-C. - XVI[e] s. apr. J.-C.). PhD Thesis, University of Nantes.
Pichard, G., Provansal, M., Sabatier, F., 2014. Les embouchures du Rhône, L'apport de la cartographie à l'étude de leur évolution géomorphologique au cours du petit âge glaciaire (PAG). Méditerranée 122, 43–59. https://doi.org/10.4000/mediterranee.6997.
Pliny the elder, n.d. Historiae Naturae/Natural History. Books 3-7, v.2, translated by Rackham, H., 1942, Loeb Classical Library, Harvard University Press, Cambridge.
Plutarch, n.d. Lives: Caius Marius. v.9. Translated by Perrin, B., 1919, Loeb Classical Library, Harvard University Press, Cambridge.
Pomey, P., Rieth, E., 2005. L'archéologie navale. Collection "Archéologiques" dirigée par Alain Ferdière, Errance.

Pomey, P., Tchernia, A., 1978. Le tonnage maximum des navires de commerce romains. Archaeonautica 2 (1), 233–251. https://doi.org/10.3406/nauti.1978.875.
Pomey, P., 1982. Le navire romain de la Madrague de Giens. Comptes rendus des séances de l'Académie des Inscriptions et Belles-Lettres, 126, 133-154. DOI: 10.3406/crai.1982.13926.
Pomponius Mela, n.d. Chorographie. Translated by Silberman, A., 1988, Les Belles Lettres, Collection des universités de France, Série latine, n° 283.
Pons, A., Toni, C., Triat, H., 1979. Édification de la Camargue et histoire holocène de sa végétation. Revue D'écologie (la Terre et La Vie) 33, 13–30. https://doi.org/10.3406/revec.1979.5169.
Provansal, M., Berger, J.-F., Bravard, J.-P., Salvador, P.-G., Arnaud-Fassetta, G., Bruneton, H., Vérot-Bourrély, A., 1999. Le régime du Rhône dans l'Antiquité et au Haut Moyen Âge : Le Rhône romain. Dynamiques fluviales, dynamiques territoriales. Gallia 56, 13–32. https://doi.org/10.3406/galia.1999.3241.
Provansal, M., Vella, C., Arnaud-Fassetta, G., Sabatier, F., Maillet, G., 2003. Rôle of fluvial sediment inputs in the mobility of the Rhône delta coast (France). Géomorphologie : Relief, Processus, Environnement 4, 271–282. https://doi.org/10.3406/morfo.2003.1190.
Purdue, L., Salomon, F., Berger, J.-F., Goiran, J.-P., 2015. Canal through time : Towards a multidisciplinary and holistic study of water systems? Water Hist. 7 (1), 1–9. https://doi.org/10.1007/s12685-015-0130-1.
Rambert, G., 1993. Le Rhône à son delta. Courrier Du Parc Naturel Régional De Camargue 41–42.
Ramsey, C.B., Lee, S., 2013. Recent and Planned Developments of the Program OxCal. Radiocarbon 55, 720–730. https://doi.org/10.1017/S0033822200057878.
Parc Naturel Régional de Camargue, 2017. Canaux et roubines de Camargue : vers une amelioration des pratiques d'entretien. Parc Naturel Régional de Camargue.
Reimer, P.J., Austin, W.E.N., Bard, E., Bayliss, A., Blackwell, P.G., Bronk Ramsey, C., Butzin, M., Cheng, H., Edwards, R.L., Friedrich, M., Grootes, P.M., Guilderson, T.P., Hajdas, I., Heaton, T.J., Hogg, A.G., Hughen, K.A., Kromer, B., Manning, S.W., Muscheler, R., Palmer, J.G., Pearson, C., van der Plicht, J., Reimer, R.W., Richards, D.A., Scott, E.M., Southon, J.R., Turney, C.S.M., Wacker, L., Adolphi, F., Büntgen, U., Capano, M., Fahrni, S.M., Fogtmann-Schulz, A., Friedrich, R., Köhler, P., Kudsk, S., Miyake, F., Olsen, J., Reinig, F., Sakamoto, M., Sookdeo, A., Talamo, S., 2020. The IntCal20 Northern Hemisphere Radiocarbon Age Calibration Curve (0-55 cal kBP). Radiocarbon 62, 725–757. https://doi.org/10.1017/RDC.2020.41.
Rey, T., 2010. Modalités du remblaiement sédimentaire des paléochenaux holocènes identifiés dans la partie occidentale du delta du Rhône (Petite Camargue, France). Quaternaire 21 (1), 11. https://doi.org/10.4000/quaternaire.5483.
Rousse, C., Marty, F., 2023. Découverte de mobilier céramique romain dans les Marais du Vigueirat (Arles) entre le port antique de Fos et le Rhône. SFECAG, Actes du congrès d'Hyères 2023.
Rousse, C., Fontaine, S., Landuré, C., Marty, F., Quesnel, Y., Vella, C., Dussouillez, P., Fleury, J., Uehara, M., 2019. Le canal de Marius : réflexions autour d'une nouvelle hypothèse de tracé dans le secteur des Marais de Vigueirat. Revue Archéologique De Narbonnaise 52, 109–146. https://doi.org/10.3406/ran.2019.1980.
Rousse, C., 2007. De la pratique à l'aménagement: la mise en valeur du milieu fluvial et lagunaire en Italie du Nord à l'époque romaine (II^e s. av. J.-C. / V^e s. ap. J.-C.). PhD Thesis, Aix-Marseille University.
Rousse, C., 2016. Ingénierie hydraulique et opérations de canalisation en Cisalpine : quels éléments de comparaison avec la Gaule Transalpine ? In: Sanchez, C., Jézégou, M.-P. (Eds.), Les ports dans l'espace méditerranéen antique : Narbonne et les systèmes portuaires fluvio-lagunaires, actes du colloque international tenu à Montpellier du 22 au 24 mai 2014, Revue Archéologique de Narbonnaise, 44, pp. 173-187.
Salomon, F., Rousse, C., 2022. Navigable canals in deltaic environments during the Roman period: deciphering location patterns. In: Lasheras González, A., Ruiz de Arbulo, J., & Terrado Ortuño, P. (Eds). Tarraco Biennal, Actes del 5^e Congrés Internacional d'Arqueologia i món antic: Ports romans. Arqueologia del sistemes portuaris. Tarragona, 24-27 de novembre de 2021. Universitat Rovira i Virgili, pp. 173-195.
Salomon, F., Rousse, C., 2023. Geoarchaeology and Archaeology of Navigable Canals in in River Deltas during the Roman Period: Technical, Methodological and Conceptual Approaches. In: Tibbs, A., Campbell, P.B. (Eds.), Rivers and Warterways in the Roman World, Empire of water. Routledge, Taylor and Francis Group, London and New-York, pp. 35-50.
Salomon, F., Purdue, L., Goiran, J.-P., Berger, J.-F., 2014. Introduction to the special issue: Roman canals studies—main research aims. Water Hist. 6, 1–9. https://doi.org/10.1007/s12685-014-0101-y.
Salomon, F., Keay, S., Carayon, N., Goiran, J.-P., 2016. The Development and Characteristics of Ancient Harbours—Applying the PADM Chart to the Case Studies of Ostia and Portus. PLoS One 11 (9), e0162587. https://doi.org/10.1371/journal.pone.0162587.
Saurel, A., 1865. "Fossae Marianae", ou Recherches sur les travaux de Marius aux embouchures du Rhône. Marseille, Roux.
Slingerland, R., Smith, N.D., 2004. River avulsions and their deposits. Annu. Rev. Earth Planet. Sci. 32, 257–285. https://doi.org/10.1146/annurev.earth.32.101802.120201.
Stanley, D.J., Warne, A.G., 1994. Worldwide Initiation of Holocene Marine Deltas by Deceleration of Sea-Level Rise. Science 265, 228–231. https://doi.org/10.1126/science.265.5169.228.
Stouff, L., 1993. La lutte contre les eaux dans les pays du bas Rhône XII^e-XV^e siècles. L'exemple Du Pays D'arles. Méditerranée 78, 57–68. https://doi.org/10.3406/medit.1993.2836.
Strabo, n.d. Geography Books 3-5, v.2. Translated by Jones, H. L., 1923, Loeb Classical Library. Loeb Classical Library, Harvard University Press, Cambridge.
Tchernia, A., 2011. Les romains et le commerce. Naples : Centre Jean Bérard, Aix-en-Provence : Centre Camille Jullian.
Tréziny, H., 2004. Sources écrites grecques et latines. In: Landuré, C., Pasqualini, M. (Eds.), Delta du Rhône. Camargue antique, médiévale et modern. Aix-en-Provence, Éditions de l'Association Provence Archéologie, pp. 93-104.
Vacchi, M., Marriner, N., Morhange, C., Spada, G., Fontana, A., Rovere, A., 2016. Multiproxy assessment of Holocene relative sea-level changes in the western Mediterranean: Sea-level variability and improvements in the definition of the isostatic signal. Earth Sci. Rev. 155, 172–197. https://doi.org/10.1016/j.earscirev.2016.02.002.
Vella, C., 1999. Perception et évaluation de la mobilité du littoral holocène sur la marge orientale du Delta du Rhône. Aix-Marseille University. PhD Thesis.
Vella, C., Bourcier, M., 1998. Stades ultimes de la montée holocène du niveau marin et subsidence tectonique dans le golfe de Fos (Provence, France)/Last stages of Holocene sea-level rise and tectonic subsidence in the Gulf of Fos (Provence, France). Géomorphologie : Relief, Processus, Environnement 4, 141–154. https://doi.org/10.3406/morfo.1998.951.
Vella, C., Landuré, C., Long, L., Dussouillez, P., Fleury, J., Tomatis, C., Sivan, O., Marty, F., Isoardi, D., Pothin, V., 2016. Ports fluviaux, ports lagunaires du Rhône et son delta pendant l'Antiquité mobilités environnementales, et dynamiques géomorphologiques comme contraintes à l'aménagement (port d'Arles, Fos/Saint-Gervais, Ulmet). In: Sanchez, C., Jézégou, M.-P. (Eds.), les ports dans l'espace méditerranéen antique : Narbonne et les systèmes portuaires fluvio-lagunaires, actes du colloque international tenu à Montpellier du 22 au 24 mai 2014, Revue Archéologique de Narbonnaise, 44, 353-368.
Vella, C., Leveau, P., Provansal, M., Gassend, J.-M., Maillet, B., Sciallano, M., 1999. Le canal de Marius et les dynamiques littorales du golfe de Fos : Le Rhône romain. Dynamiques fluviales, dynamiques territoriales. Gallia 56, 131–139. https://doi.org/10.3406/galia.1999.3250.
Vella, C., Provansal, M., 2000. Relative sea-level rise and neotectonic events during the last 6500yr on the southern eastern Rhône delta, France. Mar. Geol. 170, 27–39. https://doi.org/10.1016/S0025-3227(00)00063-3.
Vella, C., Fleury, T.-J., Raccasi, G., Provansal, M., Sabatier, F., Bourcier, M., 2005. Evolution of the Rhône delta plain in the Holocene. Mar. Geol. 222–223, 235–265. https://doi.org/10.1016/j.margeo.2005.06.028.
Vella, C., Fleury, T.J., Gensous, B., Labaune, C., Tesson, M., 2008. Grandes séquences holocènes et discontinuités sédimentaires dans le delta du Rhône. Collection EDYTEM, Cahiers De Géographie 6 (1), 155–166. https://doi.org/10.3406/edyte.2008.1036.
Véran, P., 1808. Essai sur la statistique de la ville d'Arles, son terroir et ses environs. 1^ère partie, Médiathèque d'Arles.
Verhagen, J.G.M., Kluiving, S.J., Kars, H., 2022. The option of Roman canal construction by Drusus in the Vecht river zone (the Netherlands): a geoarcheological approach. Neth. J. Geosci. 101, e4–1-23. https://doi.org/10.1017/njg.2022.2.
Viollet, P.-L., 2000. L'hydraulique dans les civilisations anciennes, 5000 d'histoire. Presses De L'école Nationale Des Ponts et Chaussées.
Wentworth, C.K., 1922. A Scale of Grade and Class Terms for Clastic Sediments. J. Geol. 30, 377–392. https://doi.org/10.1086/622910.
White, K.D., 1986. Greek and roman technology. Thames and Hudson, London.
Wikander, Ö., 2000. Handbook of ancient water technology. Technology and changes in History, 2.
Wilson, A., 2012. Water, power and culture in the Roman and Byzantine worlds : An introduction. Water History 4 (1), 1–9. https://doi.org/10.1007/s12685-012-0050-2.